Spring 2022

Controller Design for a Swirl Injection Hybrid Launch Vehicle

Ryan Kinzie
Embry-Riddle Aeronautical University, kinzier@my.erau.edu

CONTROLLER DESIGN FOR A SWIRL INJECTION HYBRID LAUNCH VEHICLE

By

Ryan Kinzie

A Thesis Submitted to the Faculty of Embry-Riddle Aeronautical University

In Partial Fulfillment of the Requirements for the Degree of

Master of Science in Aerospace Engineering

April 2022

Embry-Riddle Aeronautical University

Daytona Beach, Florida

CONTROLLER DESIGN FOR A SWIRL INJECTION HYBRID

LAUNCH VEHICLE

By

Ryan Kinzie

This Thesis was prepared under the direction of the candidate's Thesis Committee Chair, Dr. Dongeun Seo, Department of Aerospace Engineering, and has been approved by the members of the Thesis Committee. It was submitted to the Office of the Senior Vice President for Academic Affairs and Provost, and was accepted in the partial fulfillment of the requirements for the Degree of Master of Science in Aerospace Engineering.

THESIS COMMITTEE

Dongeun Seo
Digitally signed by Dongeun Seo
DN: cn=Dongeun Seo, c=US, o=Embry-Riddle Aeronautical University, ou=Aerospace Engineering Department, email=seod@erau.edu
Date: 2022.04.05 13:19:49 -04'00'

Chair, Dr. Dongeun Seo

Morad Nazari
Digitally signed by Morad Nazari
Date: 2022.04.05 19:33:08 -04'00'

Member, Dr. Morad Nazari

Richard J. Prazenica
Digitally signed by Richard J. Prazenica
Date: 2022.04.07 12:30:14 -04'00'

Member, Dr. Richard Prazenica

Daewon Kim
Digitally signed by Daewon Kim
Date: 2022.04.25 09:02:05 -04'00'

Graduate Program Coordinator,
Dr. Daewon Kim

4/25/2022

Date

Dean of the College of Engineering,
Dr. James W. Gregory

Date

Associate Provost of Academic Support,
Dr. Christopher Grant

Date

ACKNOWLEDGMENTS

First and foremost, I would like to thank my thesis advisor, Dr. Dongeun Seo, for his unwavering guidance and support throughout my time at Embry-Riddle. Without Dr. Seo's expertise and patience, this research and subsequent thesis would not have been possible.

I would also like to express my gratitude for the work of my thesis committee members, Dr. Richard Prazenica and Dr. Morad Nazari, not only for their work on my thesis, but also for their continued knowledge and instruction that has assisted me during my graduate career.

Next, I would like to thank Vaya Space for providing me with experiences, information and illustrations that have assisted and shaped my research.

Additionally, I would like to express my gratitude to Julie Joy who has provided spiritual and emotional guidance throughout the work on my thesis.

Finally, I would like to thank my whole family, including my parents, grandparents, brother and sister for their everlasting love and support.

ABSTRACT

This research is focused on the design of controllers for stabilizing a launch vehicle with an internally originating torque. The motivation for this research arises from the new development of rocket engines which swirl combustion gases to gain combustion stability benefits, and in the case of hybrid rocket engines, fuel regression benefits as well. The stability of the launch vehicle dynamics due to the internal torque has not been discussed before. To the author's knowledge, this is the first research to address the stabilization problem of the launch vehicle with internal torque. Due to the new design/characteristics of these engines, there are not many research articles on the proposed topic and the exact internal dynamics remains mostly unknown, so this research focuses on designing controllers with the ability to compensate for unknown torques. In order to develop the controllers, this research also designs a dynamics model for these launch vehicles, where the changing location of the center of mass is shown through simulation to be negligible for a real hybrid launch vehicle. Due to the proprietary nature of the exact launch vehicle data, a launch vehicle that is based on the approximate real data of a real hybrid launch vehicle was developed for the simulation of the controllers that are designed in this research. The proposed controllers include a linear quadratic regulator, PD-type controller, affine parameter-dependent Lyapunov function based controller, and an adaptive controller. These controllers must meet the goal of stabilizing the launch vehicle within the main engine's burn time. This constraint allows for these controllers to be implemented on either the first or upper stages of a launch vehicle. This research shows that the linear quadratic regulator, PD-type controller, and adaptive controller all provide adequate control over the launch vehicle with an engine originating internal toque. The performance of all four proposed controllers is demonstrated by numerical simulations. This research concludes with the recommendation of either the LQR controller or the PD-type controller for a launch vehicle similar to the one developed here. Future research may include the acquisition of real internal torque data from one of the institutions that is currently researching the design of swirl combustion engines. This data would be

used to design an internal torque model for the engine, which would then be used in the equations of motion of the launch vehicle and the subsequent controller designs.

TABLE OF CONTENTS

LIST OF FIGURES

1 Introduction

A hybrid rocket engine is an engine that uses a solid fuel and a liquid oxidizer. This is in contrast with a liquid rocket engine which uses liquid fuel and liquid oxidizer such as the main engines on the Falcon 9, and a solid rocket engine where the fuel and oxidizer are both in the solid state, such as the boosters on the Space Shuttle. Liquid rocket engines and the solid rocket engines have the richest history among the three types of engines, since almost all major launch vehicles use either one or both of these types of engines. In fact, the only hybrid rocket engine powered launch vehicles that have made it to space are the SpaceShip family of vehicles (SpaceShipOne, SpaceShipTwo), which are only capable of suborbital space flights. Due to the rarity of hybrid rocket engine powered launch vehicles, research into hybrid rocket engines has been largely scarce [1]. One of the factors that has played into the rarity of hybrid rocket engines on launch vehicles is that hybrid rocket engines experience combustion instabilities. These instabilities arise partially from the fact that the fuel and oxidizer of a hybrid rocket engine are in two different states of matter. Therefore, before the fuel can burn, the fuel needs to melt, be vaporized, and then mix with the already gaseous oxidizer [1]. Additional problems, such as uneven fuel regression within a hybrid arise as well since the fuel at the injector end of the combustion chamber will burn at a greater rate than the fuel located further from the injector. As the gases accelerate through the combustion chamber, a boundary layer is created on the wall of the fuel grain that prohibits the melting of the fuel grain, making the fuel regression rate a function of the axial location within the combustion chamber [1]. Uneven fuel regression is an issue since fuel will remain within the combustion camber that cannot be burned, which reduces the efficiency of the engine, and adds weight to the dry mass of the launch vehicle. Figure 1.1 presents a cutaway diagram of a typical hybrid rocket engine.

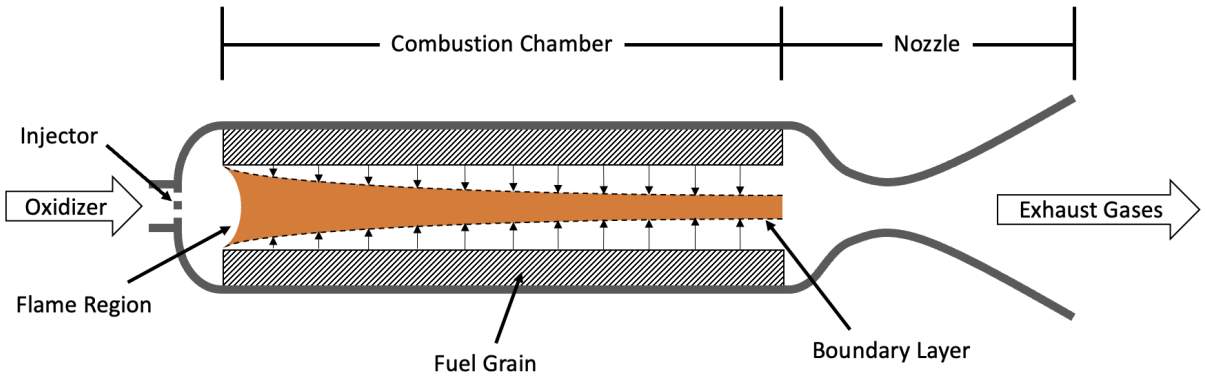

Figure 1.1 Hybrid Rocket Engine Cut Away View

Solving combustion instabilities and uneven fuel grain regression have become critical areas of interest to multiple aerospace companies involved in the manufacturing of hybrid and liquid rocket engines [2, 3]. Through research, companies have proven that the swirling of combustion gases alleviates these problems [4–6]. The swirling of the combustion gases is accomplished by injecting the oxidizer and/or fuel into the rocket engine's combustion chamber at carefully calculated angles to cause the combustion gases of the rocket's engines to swirl around the interior of the combustion chambers numerous times before entering the throat of the engine's nozzle. Because the swirling motion of the combustion gases is significant, there is a potential for the gases to impose a distributed force along the wall of the combustion chambers of these rocket engines. Additionally, there is also a potential for the gases to continue swirling when ejected from the diverging section of the nozzle. Figure 1.2 presents a computer-aided design rendering of the Vaya Space's hybrid rocket engine with combustion path lines illustrated, courtesy of Vaya Space.

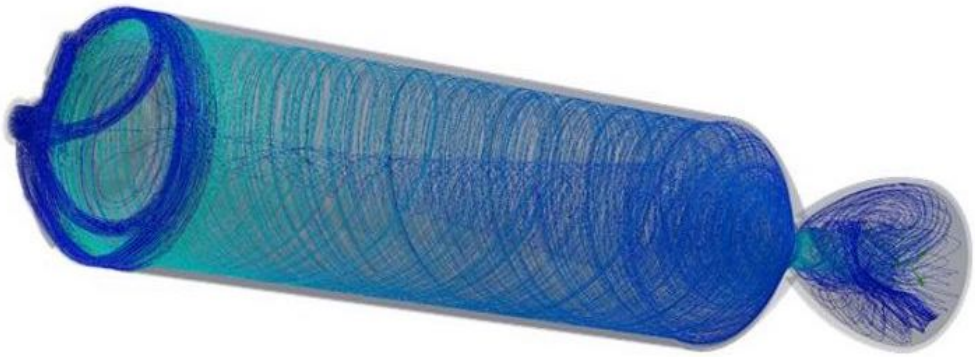

Figure 1.2 Vaya Space's Hybrid Rocket Engine with Combustion Gas Path Lines

Although ground based swirl combustion engines have been successfully tested [2, 3], the internally generated torques are unknown. Additionally, there has only been one successful launch of a launch vehicle that swirls its combustion gases in the manner depicted by Figure 1.2 to the extent of the author's knowledge. Due to the unknown dynamics of swirl combustion engines, this research puts significant weight on designing a controller that is robust enough to compensate for the unknown dynamics, since these dynamics pose the risk of causing the launch vehicle to begin spinning uncontrolled about its minor-axis (the axis running from the nose of the rocket to the center of its engine). A minor-axis spinner is inherently unstable since any perturbations will cause the spinner to oscillate until it begins spinning about its major axis.

The objective of this research is to design a simple and robust controller that has the potential to be implemented on one of these early launch vehicles. Additionally, the controller must stabilize the launch vehicle within the thirty-second burn time of the main engine. This burn time constraint allows the controller designed in this thesis to be applied to both the first and upper stages of a launch vehicle.

2 Literature Review and Preliminaries

This section details the previous works that were utilized to begin the research of controlling a launch vehicle with internal torque. Then, a review of the Linear Time-Invariant (LTI) controller is presented, which feeds into the review of the Linear-Quadratic Regulator (LQR), and the review of the PD-type controller. Lastly, a review of the Gain-Scheduled controller is presented and followed by reviews of nonautonomous system stability, Lyapunov functions, and Barbalat's Lemma, which are essential knowledge for the design of the Gain-Scheduled controller and stability proofs of the controllers formulated in this research.

2.1 Launch Vehicles with Internal Torque

Besides the work conducted by Kinzie and Seo [7], there has been no research to the extent of the author's knowledge on controller design for a launch vehicle with an internally originating torque. This is likely due to the fact that the research into swirl combustion engines is relatively new, with only a single launch of a vehicle which contains one of these engines. In fact, literature detailing controller design of any launch vehicle is not plentiful on the whole due to the fact that the vast majority of institutions that research launch vehicle controls are the companies that manufacture those vehicles. There are some works that detail these controller designs, such as that by Wie and Whorton [8]. However, most of the research on launch vehicle controller design is proprietary and not accessible to the public. Instead, it is recommended to research control solutions for missiles, since the controls problem between missiles and launch vehicles is nearly identical, and is more readily available than the research for launch vehicles. Zipfel has a wealth of information on the topic of missile control with references that range from equation of motion derivation [9], Schmitt triggers and controller design [10], to the more advanced modeling of optimal trajectories for a vehicle to orbit [11]. Even though this research does not go into detail about the aerodynamics equations that affect launch vehicles in the atmosphere, a great reference for these aerodynamics equations is the work by Fleeman [12]. This reference also covers static stability and how to design the aerosurfaces on a vehicle, which is an important concept for launch vehicle designers.

2.2 Linear Time-Invariant Controllers

It is assumed that the desired controller to achieve the control objective will be an LTI controller. Previous research on LTI controllers have proven that these controllers provide a simple robust control solution for systems with unknown dynamics [13–15]. Although this research specifies that LTI controllers are not guaranteed to provide a robust solution for time-varying systems with undefined dynamics, this paper's research assumes that because the launch vehicle's system is only changing as a function of the vehicle's depleting mass, which is a known function of time, an LTI controller is able to achieve the stability goal. This research assumes that an LTI controller designed at either the initial state or final state of the launch vehicle will provide the desired simple and robust control.

2.3 Linear-Quadratic Regulator

The LQR's inherent robustness with respect to uncertainties makes the controller of particular interest for this research [16–21]. Additionally, this research expects that the LQR controller's ability to optimally control either a time-varying or time-invariant system may give the LQR controller the ability to achieve the stability goal. It is expected that an LQR controller designed at either the initial state or final state of the vehicle will be able to provide the desired control over the launch vehicle.

2.4 PD-type Controller

In addition to the LQR controller, a PD-type controller is developed and compared against the LQR controller. The PD-type controller is relatively simple and has proven robustness in past research [22–25]. Therefore, it is assumed that the PD-type controller will provide a strong comparison against the LQR controller.

2.5 Gain-Scheduled Controller

The gain-scheduled controller approach proposed in this work is an affine parameter-dependent Lyapunov function based controller which involves the direct synthesis of a controller rather than from a set of local linear controllers [26]. Affine parameter-dependent

Lyapunov function based controllers guarantee stability for all values of specified parameters, as opposed to interpolation based gain scheduling methods which may create controllers that do not guarantee stability for the interpolated points between sets of local linear controllers [27]. Since affine parameter-dependent Lyapunov function based controllers account for parameter variation, this research expects that this type of controller will be able to adequately control the launch vehicle when the Lyapunov function is affinely dependent on the mass of the launch vehicle.

2.6 Nonautonomous System Stability

Nonautonomous systems are functions of an independent variable which is not dependent on the state of the system [28]. Since the mass of the launch vehicle will deplete as a function of time independent of the states of the launch vehicle, the system is considered nonautonomous. The mass function is described in more detail in Section 3.1 of this thesis. For the time-varying (nonautonomous) system,

$$\dot{\vec{x}} = \vec{f}\left(\vec{x}, t\right), \quad \vec{x} \in \mathbb{R}^n$$

where $\vec{x}\left(t_0\right) = \vec{x}_0$, the system has an equilibrium point if,

$$\vec{f}\left(\vec{x}^*, t\right) = \vec{0} \quad \forall \quad t \geq t_0$$

The conditions for stability and asymptotic stability of a nonautonomous system's equilibrium points largely remain the same as those for an autonomous system. However, the solution for a nonautonomous system depends on t_0 and t, while an autonomous system's solution only depends on $(t - t_0)$. This means that the stability of $\vec{x}^*$ may depend on t_0 [28]. As stated by Khalil [28],

- The equilibrium point, $\vec{x}^*$ is *stable* if, $\forall\ \varepsilon > 0$, $\exists\ \delta\left(\varepsilon, t_0\right) > 0$ such that,

$$\left\|\vec{x}\left(t_0\right)\right\| < \delta, \quad \left\|\vec{x}\left(t\right)\right\| < \varepsilon, \quad \forall \quad t \geq t_0 \geq 0$$

For the time-varying case it is possible for the constant δ to depend on t_0.

- The equilibrium point is *uniformly stable* if $\forall\ \varepsilon > 0$, $\exists\ \delta(\varepsilon) > 0$ independent of t_0, such that the above inequality is satisfied.

- The equilibrium point is *asymptotically stable* if it is stable and $\exists\ \delta(t_0) > 0$ such that $\vec{x}(t) \to \vec{x}^*$ as $t \to \infty\ \forall\ \|\vec{x}(t)\| < \delta(t_0)$. Here, $\delta(t_0)$ is a constant that depends on t_0.

- The equilibrium point is *uniformly asymptotically stable* if it uniformly stable and $\exists$ $c > 0$, independent of t_0, such that $\forall\ \|\vec{x}(t_0)\| < c$, $\vec{x}(t) \to \vec{x}^*$ as $t \to \infty$ uniformly in t.

- The equilibrium point is *globally uniformly asymptotically stable*, if it is uniformly stable, $\delta(\varepsilon)$ can be chosen to satisfy $\lim_{\varepsilon\to\infty} \delta(\varepsilon) = \infty$ and for each pair of positive numbers, c and η, $\exists\ T(c,\eta)$ such that,

$$\|\vec{x}(t)\| < \eta \quad \forall \quad t \geq t_0 + T(c,\eta), \quad \forall \quad \|\vec{x}(t_0)\| < c$$

These stability conditions for nonautonomous systems may then be extended to Lyapunov functions [28].

2.7 Lyapunov Functions

In 1892, Aleksandr Lyapunov proved that functions related to the energy of a system (now known as Lyapunov Functions) may predict the stability of the equilibrium points of a system [28]. For a system of ordinary differential equations that does not explicitly depend on independent variables (autonomous system),

$$\dot{\vec{x}} = \vec{f}(\vec{x})$$

Let $V(\vec{x})$ be a positive definite, continuously differentiable function within the domain $D \subset R^n$. By definition, $V(\vec{x})$ is a positive definite function if $V\left(\vec{0}\right) = \vec{0}$ *and* $V(\vec{x}) > \vec{0}\ \ \forall\ \ \vec{x} \neq \vec{0}, \vec{x} \in D$ [28]. Lyapunov stability theorem then states

that if $V(\vec{x})$ is a positive definite function for the equilibrium point $\vec{x} = \vec{0}$ within D , and

$$\dot{V}(\vec{x}) \leq \vec{0} \quad \forall \quad \vec{x} \in D$$

is true, then $\vec{x} = \vec{0}$ is stable. Additionally, if

$$\dot{V}(\vec{x}) < \vec{0} \quad \forall \quad \vec{x} \neq \vec{0}, \vec{x} \in D$$

holds true, then $\vec{x} = \vec{0}$ is an asymptotically stable equilibrium of the system [28]. These basic stability conditions for the autonomous system may be extended to nonautonomous systems through the analysis of decrescent Lyapunov functions. A candidate Lyapunov function, $V(\vec{x}, t)$ where $V(\vec{0}, t) = 0$, is decrescent for a time-varying system if $V(\vec{x}, t) \leq W(\vec{x})$ where $W(\vec{x})$ is some positive definite function. Additionally, if $0 < V(\vec{x}, t) \leq W(\vec{x})$ then the candidate Lyapunov function is a positive definite, decrescent function.

Using decrescent Lyapunov functions, Lyapunov's direct method may be used to analyze the stability of nonautonomous systems. From Khalil [28],

- The equilibrium point $\vec{x}^* = \vec{0}$ is *uniformly stable* within the region, $D \subset \mathbb{R}^n$ if there exists a positive definite, decrescent function such that,

$$W_1(\vec{x}) \leq V(\vec{x}, t) \leq W_2(\vec{x})$$

$$\dot{V}(\vec{x}, t) = \frac{\partial V}{\partial t} + \left(\frac{\partial V}{\partial \vec{x}}\right)^T \vec{f}(\vec{x}, t) \leq 0$$

$\forall\ \vec{x}(t) \in D$ and $t \geq 0$, where $W_1(\vec{x})$ and $W_2(\vec{x})$ are continuous positive definite functions on D.

- The equilibrium point is *uniformly asymptotically stable* in the region D if $\dot{V}(\vec{x}, t) \leq -W_3(\vec{x})\ \forall\ \vec{x}(t) \in D$ and $t \geq 0$, where $W_3(\vec{x})$ is a continuous positive definite function on D.

- The equilibrium point is *globally uniformly asymptotically stable* if $\dot{V}(\vec{x},t) \leq -W_3(\vec{x})$ $\forall\ \vec{x}(t) \in \mathbb{R}^n\ (D=\mathbb{R}^n),\ t \geq 0$, and $W_1(\vec{x})$ is radially unbounded. That is, $\lim_{\vec{x}\to\infty} W_1(\vec{x}) = \infty$.

The affine parameter-dependent Lyapunov function based controller designed in this research will guarantee the stability of nonautonomous systems through linear parameter-varying (LPV) Lyapunov functions. These LPV Lyapunov functions are able to guarantee stability by proving that the derived controller is able to make the system meet one or more of the Lyapunov stability conditions for a nonautonomous system.

2.8 Barbalat's Lemma

Barbalat's Lemma is often used in conjunction with Lyapunov's Direct method for nonautonomous systems when $\dot{V}(\vec{x},t)$ can only be shown to be negative semi-definite. The lemma is stated as follows;

If $lim_{t\to\infty} \int_0^t f(\tau)\,d\tau$ exists and is finite for a uniformly continuous function, $f(t)$, and if $\dot{f}(t)$ is uniformly continuous, then $f(t) \to 0$ as $t \to \infty$ [28, 29].

3 Problem Formulation

In this chapter, the dynamics model of the launch vehicle and the designs of the controllers will be introduced. First, a model for the changing mass of the launch vehicle and the vehicle's linear and angular equations of motion will be derived. Then, the LQR controller is derived, followed by the PD-type controller. Next, the affine-parameter dependent Lyapunov function based control is derived, followed by the derivation of the adaptive controller. Each derivation is followed with a stability proof for the controller, or in the case of the adaptive controller, the Lyapunov stability proof is utilized in the derivation of the controller.

3.1 Changing Mass

As the launch vehicle ascends, its mass will change as a function of time since the fuel and oxidizer stored on the launch vehicle will be burned off to generate the thrust of the rocket. One of the advantages of the swirl injection hybrid rocket engines is that the mass flow rate (time rate of change of the mass), $\dot{m}$, remains constant for a constant throttle setting. This is a highly desired characteristic of rocket engines since there is no decrease in thrust as the engine burns, which is a common occurrence in conventional hybrid and solid rocket engines. Since $\dot{m}$ is constant, and the initial mass of the launch vehicle, m_0, is known, the time-dependent mass of the launch vehicle, $m(t)$, is a known linear function. Therefore, $m(t)$ will take the form,

$$m(t) = \dot{m}t + m_0 \tag{3.1}$$

Since the mass of the launch vehicle is a function of time, the location of the center of mass of the launch vehicle will also change as a function of time. To determine if this effect is neglectable, a model was created to simulate the change of the location of the center of mass of the launch vehicle based on properties from an actual hybrid rocket engine powered launch vehicle. Presented in Figure 3.1 is an illustration of a hybrid rocket engine powered launch vehicle with the oxidizer tank and fuel grain displayed.

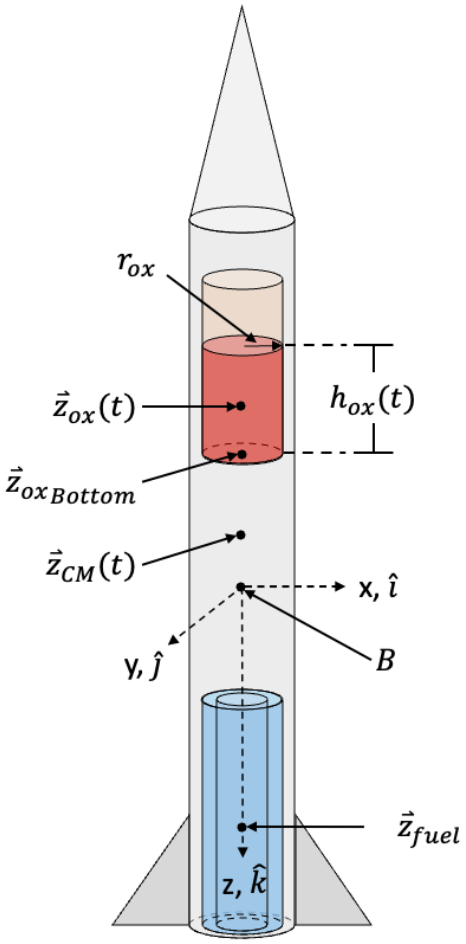

Figure 3.1 Hybrid Launch Vehicle with Oxidizer Tank and Fuel Grain Shown

In Figure 3.1, various dimensions are shown which aided in deriving the calculations for determining the location of the center of mass of the launch vehicle. Here, $\vec{z}_{CM}(t)$ is the location of the time-dependent center of mass of the launch vehicle, $\vec{z}_{ox}(t)$ is the location of the time-dependent center of mass of oxidizer tank, $\vec{z}_{ox_{Bottom}}$ is the the location of the bottom of the oxidizer tank, and $\vec{z}_{fuel}$ is the location of the center of mass of the fuel grain. All four of these points are measured with respect to B, which is the origin of the launch vehicle's Body-Fixed Frame $(\hat{\imath}, \hat{\jmath}, \hat{k})$. Because swirl injection hybrid rocket engines reduce uneven fuel regression to a neglectable amount, it is assumed that $\vec{z}_{fuel}$ is a constant value. Additionally, the mass of the oxidizer and the fuel grain, $m_{ox}(t)$ and $m_{fuel}(t)$, respectively, are known functions of time.

A simple relation can then be made to determine the center of mass between the oxidizer tank and the fuel grain (which we will call $\vec{z}_{CM_{propellant}}(t)$) by multiplying the mass of each by their respective location relative to the Body-Fixed Frame and then dividing by the total mass of the propellants,

$$\vec{z}_{CM_{propellant}}(t) = \frac{m_{fuel}(t)\,\vec{z}_{fuel} + m_{ox}(t)\,\vec{z}_{ox}(t)}{m_{fuel}(t) + m_{ox}(t)} \tag{3.2}$$

Then, $\vec{z}_{CM}(t)$ can be determined in a similar way by multiplying the total mass of the propellants by $\vec{z}_{CM_{propellant}}(t)$, and then adding the product to the product of the dry mass of the launch vehicle, m_f, multiplied by the location of the dry center of mass of the launch vehicle with respect to the Body-Fixed Frame, $\vec{z}_{CM_f}$, all divided by the total mass of the launch vehicle,

$$\vec{z}_{CM}(t) = \frac{(m_{fuel}(t) + m_{ox}(t))\,\vec{z}_{CM_{propellant}}(t) + m_f\vec{z}_{CM_f}}{m_{fuel}(t) + m_{ox}(t) + m_f}$$

Here, it is assumed that the entirety of the propellants will be used up during the engine's burn which allows the dry mass and dry center of mass of the launch vehicle to be set equal to the final values of $m(t)$ and $\vec{z}_{CM}(t)$; hence, the subscript f. Then, $\vec{z}_{CM_f} = \vec{0}$, which makes the vector coincide with the Body-Fixed Frame of the launch vehicle and provides the simplified equation,

$$\vec{z}_{CM}(t) = \frac{(m_{fuel}(t) + m_{ox}(t))\,\vec{z}_{CM_{propellant}}(t)}{m_{fuel}(t) + m_{ox}(t) + m_f} \tag{3.3}$$

Next, the center of mass of the oxidizer tank is calculated by assuming the oxidizer tank to be cylindrical. The volume of the oxidizer within the tank is then,

$$V_{ox}(t) = \pi r_{ox}^2 h_{ox}(t)$$

where, $h_{ox}(t)$ is the time-dependent height of the oxidizer within the oxidizer tank and r_{ox} is the radius of the oxidizer tank. The volume of oxidizer within the tank is also equal to the mass of the oxidizer divided by the density of the oxidizer, ρ_{ox}, which is a known constant value,

$$V_{ox}(t) = \frac{m_{ox}(t)}{\rho_{ox}}$$

Equating these two expressions and solving for the height of the oxidizer yields,

$$h_{ox}(t) = \frac{m_{ox}(t)}{\pi r_{ox}^2 \rho_{ox}}$$

The location of the center of mass of the oxidizer with respect to the Body-Fixed Frame is then very simply $\vec{z}_{ox_{Bottom}}$ minus half the height of the oxidizer,

$$\vec{z}_{ox}(t) = \vec{z}_{ox_{Bottom}} - \frac{m_{ox}(t)}{2\pi r_{ox}^2 \rho_{ox}} \tag{3.4}$$

Substituting Eq. (3.2) and Eq. (3.4) into Eq. (3.3) yields,

$$\vec{z}_{CM}(t) = \frac{m_{fuel}(t)\,\vec{z}_{fuel} + m_{ox}(t)\left(\vec{z}_{ox_{Bottom}} - \frac{m_{ox}(t)}{2\pi r_{ox}^2 \rho_{ox}}\right)}{m_{fuel}(t) + m_{ox}(t) + m_f}$$

Lastly, it is necessary to relate the change of the location of the center of mass with the length of the launch vehicle. This will be expressed as the percentage of the difference between the Body-Fixed Frame and $\vec{z}_{CM}(t)$ with respect to the length of the launch vehicle,

$$\vec{z}_{CM_{Percentage}}(t) = \frac{-\vec{z}_{CM}(t)}{\text{length of vehicle}} \times 100 \tag{3.5}$$

Figure 3.2 presents the plot of $\vec{z}_{CM_{Percentage}}(t)$ verse time. The values used for this simulation are real values from a designed and build hybrid rocket. However, due to the proprietary nature of the information, none of the values will be shared in this research. These values are not significant though, because the only information needed for this research is how the

location of the center of mass of a hybrid rocket engine powered launch vehicle changes with respect to the launch vehicle's length over time. From this figure, it is easy to see that the location of the center of mass of the hybrid launch vehicle changes very little over the course of an engine burn (maximum of $< 3\%$). Therefore, for the remainder of this research, it is assumed that the center of mass of the launch vehicle is located constantly at the origin of the launch vehicle's Body-Fixed Frame.

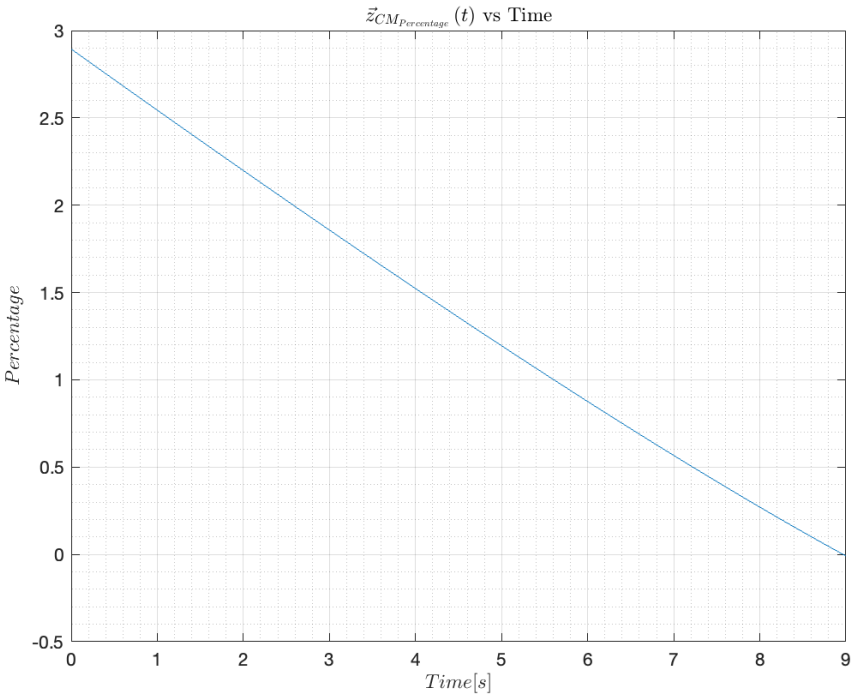

Figure 3.2 $\vec{z}_{CM_{Percentage}}(t)$ vs Time

3.2 Equations of Motion

Figure 3.3 illustrates the Body-Fixed Frame in relation to the Local-Level Frame ($\hat{I}$, $\hat{J}$, $\hat{K}$), where $\vec{S}(t)$ is the position vector between the two frames of reference.

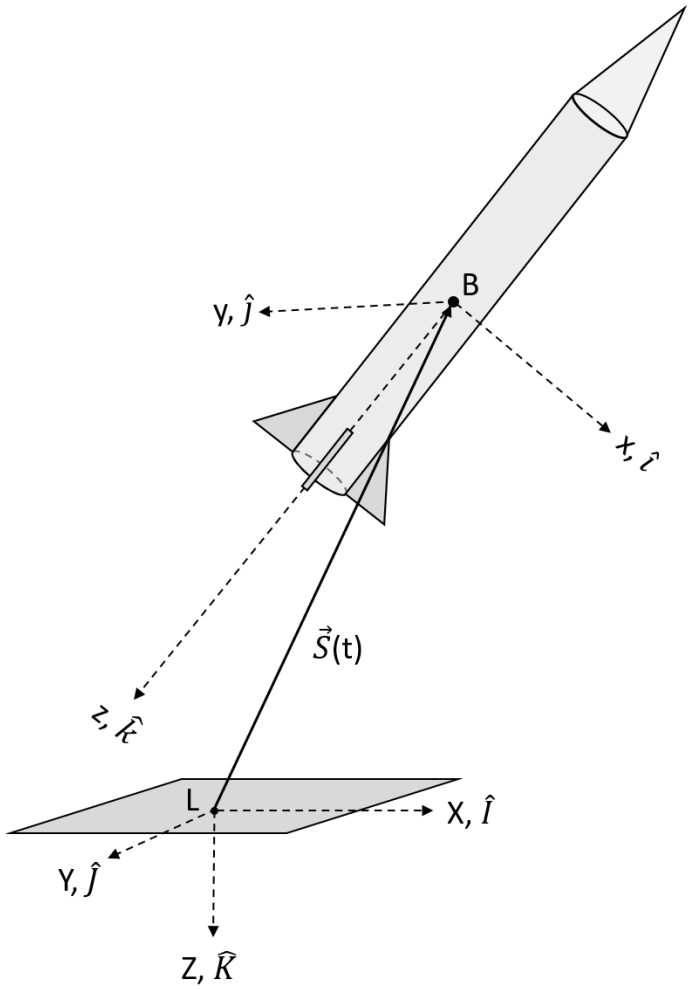

Figure 3.3 Launch Vehicle Frames of Reference

The six-degree-of-freedom nonlinear rigid-body equations of motion, as observed in the Body-Fixed Frame, are derived directly from Zipfel's work [9] as,

$$m\left(t\right)\dot{\vec{v}}^{B}\left(t\right)+m\left(t\right)\left(\vec{\omega}^{B}\left(t\right)\times\vec{v}^{B}\left(t\right)\right)=\vec{F}_{Aerodynamic}^{B}\left(t\right)+\vec{F}_{Thrust}^{B}\left(t\right)+m\left(t\right)\left[T\left(t\right)\right]^{BL}\vec{g}^{L}\left(t\right)$$

$$\dot{\vec{S}}^{L}\left(t\right)=\left[T\left(t\right)\right]^{BL^{T}}\vec{v}^{B}\left(t\right)$$

$$\left[I\left(t\right)\right]^{B}\dot{\vec{\omega}}^{B}\left(t\right)+\vec{\omega}^{B}\left(t\right)\times\left[I\left(t\right)\right]^{B}\vec{\omega}^{B}\left(t\right)=\vec{M}_{Aerodynamic}^{B}\left(t\right)+\vec{M}_{Thrust}^{B}\left(t\right)$$

$$[T(t)]^{BL} = \begin{bmatrix} q_0^2(t) + q_1^2(t) - q_2^2(t) - q_3^2(t) & 2(q_1(t)\,q_2(t) + q_0(t)\,q_3(t)) & 2(q_1(t)\,q_3(t) - q_0(t)\,q_2(t)) \\ 2(q_1(t)\,q_2(t) - q_0(t)\,q_3(t)) & q_0^2(t) - q_1^2(t) + q_2^2(t) - q_3^2(t) & 2(q_2(t)\,q_3(t) + q_0(t)\,q_1(t)) \\ 2(q_1(t)\,q_3(t) + q_0(t)\,q_2(t)) & 2(q_2(t)\,q_3(t) - q_0(t)\,q_1(t)) & q_0^2(t) - q_1^2(t) - q_2^2(t) + q_3^2(t) \end{bmatrix}$$

$$\begin{Bmatrix} \dot{q}_0(t) \\ \dot{q}_1(t) \\ \dot{q}_2(t) \\ \dot{q}_3(t) \end{Bmatrix} = \frac{1}{2} \begin{bmatrix} 0 & -\omega_1(t) & -\omega_2(t) & -\omega_3(t) \\ \omega_1(t) & 0 & \omega_3(t) & -\omega_2(t) \\ \omega_2(t) & -\omega_3(t) & 0 & \omega_1(t) \\ \omega_3(t) & \omega_2(t) & -\omega_1(t) & 0 \end{bmatrix} \begin{Bmatrix} q_0(t) \\ q_1(t) \\ q_2(t) \\ q_3(t) \end{Bmatrix}$$

with $\vec{\omega}^B(t) = [\omega_1(t), \omega_2(t), \omega_3(t)]^T$. Here, $\vec{F}^B(t)$ and $\vec{M}^B(t)$ are force and applied moment, $\vec{v}^B(t)$ and $\vec{\omega}^B(t)$ are linear and angular velocity, and $m(t)$ and $[I(t)]^B$ are mass and moment of inertia, respectively. $[T(t)]^{BL}$ is the quaternion-based rotation matrix from the Body-Fixed Frame to the Local-Level Frame, where $q_i(t)$ denotes the i^{th} element of the quaternion vector, $\vec{q}(t)$. The scalar part of $\vec{q}(t)$ is denoted by $i = 0$ while the vector part is denoted by $i = 1, 2, 3$. Lastly, $\vec{g}^L(t)$ is the gravitational acceleration vector, which is equal to $\vec{g}^L(t) = [0, 0, g]^T$. The superscripts B and L denote that the respective vector is resolved in either the Body-Fixed Frame or the Local-Level Frame, respectively.

For this research, the rigid-body equations of motion from Zipfel's work are altered by considering the moment of inertia of the launch vehicle as a function of time since the moment of inertia of the launch vehicle is a function of its mass, which will change as the fuel and oxidizer in the launch vehicle are burned. Additionally, we do not consider the aerodynamic forces nor the aerodynamic moment applied to the launch vehicle since we are generalizing this problem for the first and upper stages of a launch vehicle. Lastly, the linear position of the launch vehicle, $\dot{\vec{S}}^B(t)$, is resolved in the Body-Fixed Frame instead of the Local-Level Frame.

These alterations provide the six-degree-of-freedom nonlinear rigid-body equations of motion as observed in the Body-Fixed Frame that are used for the simulations of the launch vehicle.

$$m(t)\,\dot{\vec{v}}^{B}(t) = \vec{F}^{B}_{Thrust}(t) + m(t)\,[T(t)]^{BL}\,\vec{g}^{L}(t) - \dot{m}\vec{v}^{B}(t) - m(t)\left(\vec{\omega}^{B}(t) \times \vec{v}^{B}(t)\right) \quad (3.6)$$

$$\dot{\vec{S}}^{B}(t) = \vec{v}^{B}(t) \quad (3.7)$$

$$[I(t)]^{B}\,\dot{\vec{\omega}}^{B}(t) = -\left[\dot{I}\right]^{B}\vec{\omega}^{B}(t) - \vec{\omega}^{B}(t) \times [I(t)]^{B}\,\vec{\omega}^{B}(t) + \vec{M}^{B}(t) \quad (3.8)$$

$$[T(t)]^{BL} = \begin{bmatrix} q_0^2(t) + q_1^2(t) - q_2^2(t) - q_3^2(t) & 2(q_1(t)\,q_2(t) + q_0(t)\,q_3(t)) & 2(q_1(t)\,q_3(t) - q_0(t)\,q_2(t)) \\ 2(q_1(t)\,q_2(t) - q_0(t)\,q_3(t)) & q_0^2(t) - q_1^2(t) + q_2^2(t) - q_3^2(t) & 2(q_2(t)\,q_3(t) + q_0(t)\,q_1(t)) \\ 2(q_1(t)\,q_3(t) + q_0(t)\,q_2(t)) & 2(q_2(t)\,q_3(t) - q_0(t)\,q_1(t)) & q_0^2(t) - q_1^2(t) - q_2^2(t) + q_3^2(t) \end{bmatrix} \quad (3.9)$$

$$\begin{Bmatrix} \dot{q}_0(t) \\ \dot{q}_1(t) \\ \dot{q}_2(t) \\ \dot{q}_3(t) \end{Bmatrix} = \frac{1}{2}\begin{bmatrix} 0 & -\omega_1(t) & -\omega_2(t) & -\omega_3(t) \\ \omega_1(t) & 0 & \omega_3(t) & -\omega_2(t) \\ \omega_2(t) & -\omega_3(t) & 0 & \omega_1(t) \\ \omega_3(t) & \omega_2(t) & -\omega_1(t) & 0 \end{bmatrix}\begin{Bmatrix} q_0(t) \\ q_1(t) \\ q_2(t) \\ q_3(t) \end{Bmatrix} \quad (3.10)$$

3.3 Linearization

The first step in designing the four controllers (LQR, PD-type, affine parameter dependent Lyapunov-function based, and adaptive) is to linearize the nonlinear model of the launch vehicle. The goal of linearization is to simplify the system model so that an input to the system will provide a predictable output, which is not true for nonlinear systems.

3.3.1 Linearization of Quaternions

The linearized quaternion rotational matrix is equal to a small change in the rotational matrix, $[\delta T(t)]^{BL}$, multiplied to its previous iteration, $[T(t)]^{BL}_{i-1}$ [30],

$$[T(t)]^{BL} = [\delta T(t)]^{BL}\,[T(t)]^{BL}_{i-1}$$

Here, $[\delta T(t)]^{BL}$ is equivalent to the small angle approximation of an $\hat{i}, \hat{j}, \hat{k}$ rotational matrix using Euler Angles, where $\psi(t)$, $\theta(t)$ and $\phi(t)$ are the roll, pitch, and yaw angles, respectively.

$$[\delta T(t)]^{BL} \approx \begin{bmatrix} 1 & \delta\phi(t) & -\delta\theta(t) \\ -\delta\phi(t) & 1 & \delta\psi(t) \\ \delta\theta(t) & -\delta\psi(t) & 1 \end{bmatrix}$$

Then, $[T(t)]_{i-1}^{BL}$ is given by,

$$[T(t)]_{i-1}^{BL} = \begin{bmatrix} T_{i-1_{11}}(t) & T_{i-1_{12}}(t) & T_{i-1_{13}}(t) \\ T_{i-1_{21}}(t) & T_{i-1_{22}}(t) & T_{i-1_{23}}(t) \\ T_{i-1_{31}}(t) & T_{i-1_{32}}(t) & T_{i-1_{33}}(t) \end{bmatrix} = \begin{bmatrix} 1 & 0 & 0 \\ 0 & 1 & 0 \\ 0 & 0 & 1 \end{bmatrix}$$

Therefore, the linearization of $[T(t)]^{BL}$ follows as,

$$[T(t)]^{BL} = \begin{bmatrix} 1 & \delta\phi(t) & -\delta\theta(t) \\ -\delta\phi(t) & 1 & \delta\psi(t) \\ \delta\theta(t) & -\delta\psi(t) & 1 \end{bmatrix}$$

3.3.2 Linearization of Equations of Motion

To aid in the linearization of the equations of motion of the launch vehicle, Eqs. (3.6) and (3.8) are expanded out. The expansion of Eq. (3.6) yields,

$$\begin{aligned} m(t)\dot{v}_x &= F_{Thrust_x}(t) - m(t)g\delta\theta - \dot{m}v_x(t) - m(t)(\omega_y(t)v_z(t) - \omega_z(t)v_y(t)) \\ m(t)\dot{v}_y &= F_{Thrust_y}(t) + m(t)g\delta\psi - \dot{m}v_y(t) - m(t)(\omega_z(t)v_x(t) - \omega_x(t)v_z(t)) \\ m(t)\dot{v}_z &= F_{Thrust_z}(t) + m(t)g - \dot{m}v_z(t) - m(t)(\omega_x(t)v_y(t) - \omega_y(t)v_x(t)) \end{aligned} \tag{3.11}$$

For this research, it is assumed that the launch vehicle is axi-symmetric about the $\hat{k}$ axis; therefore, Eq. (3.8) is expanded with the assumption that $I_{xx}(t) = I_{yy}(t)$. Additionally, the

moment vector, $\vec{M}^{B}(t)$, is a sum of the internal moments that are produced by the engine, $\vec{M}_{Int}(t)$, and the control torque vector, $\vec{U}(t)$. This yields,

$$\begin{aligned} I_{xx}(t)\dot{\omega}_x(t) &= -\dot{I}_{xx}\omega_x(t) - (I_{zz}(t) - I_{xx}(t))\,\omega_y(t)\,\omega_z(t) + M_{Int_x}(t) + U_x(t) \\ I_{xx}(t)\dot{\omega}_y(t) &= -\dot{I}_{xx}\omega_y(t) - (I_{xx}(t) - I_{zz}(t))\,\omega_x(t)\,\omega_z(t) + M_{Int_y}(t) + U_y(t) \\ I_{zz}(t)\dot{\omega}_z(t) &= -\dot{I}_{zz}\omega_z(t) + M_{Int_z}(t) + U_z(t) \end{aligned} \tag{3.12}$$

The moments of inertia are easily found by using the equations for the moments of inertia of a cylinder, $I_{xx}(t) = \frac{1}{4}m(t)\,r^2 + \frac{1}{12}m(t)\,l^2$ and $I_{zz}(t) = \frac{1}{2}m(t)\,r^2$. Here, r and l are the radius length of the launch vehicle, respectively. The time derivatives of the moments of inertia are very simply the constant values, $\dot{I}_{xx} = \frac{1}{4}\dot{m}r^2 + \frac{1}{12}\dot{m}l^2$ and $\dot{I}_{zz} = \frac{1}{2}\dot{m}r^2$. Plugging the moments of inertia and their derivatives into Eq. (3.12) provides the following,

$$\begin{aligned} \left(\frac{1}{4}m(t)\,r^2 + \frac{1}{12}m(t)\,l^2\right)\dot{\omega}_x(t) = &-\left(\frac{1}{4}\dot{m}r^2 + \frac{1}{12}\dot{m}l^2\right)\omega_x(t) - \left(\left(\frac{1}{2}m(t)\,r^2\right) - \left(\frac{1}{4}m(t)\,r^2\right.\right. \\ &\left.\left. + \frac{1}{12}m(t)\,l^2\right)\right)\omega_y(t)\,\omega_z(t) + M_{Int_x}(t) + U_x(t) \\ \left(\frac{1}{4}m(t)\,r^2 + \frac{1}{12}m(t)\,l^2\right)\dot{\omega}_y(t) = &-\left(\frac{1}{4}\dot{m}r^2 + \frac{1}{12}\dot{m}l^2\right)\omega_y(t) - \left(\left(\frac{1}{4}m(t)\,r^2 + \frac{1}{12}m(t)\,l^2\right)\right. \\ &\left. - \left(\frac{1}{2}m(t)\,r^2\right)\right)\omega_x(t)\,\omega_z(t) + M_{Int_y}(t) + U_y(t) \\ \left(\frac{1}{2}m(t)\,r^2\right)\dot{\omega}_z(t) = &-\left(\frac{1}{2}\dot{m}r^2\right)\omega_z(t) + M_{Int_z}(t) + U_z(t) \end{aligned}$$

After simplification, the fully expanded form of the equations is obtained as,

$$
\begin{aligned}
m(t)\left(\frac{1}{4}r^2+\frac{1}{12}l^2\right)\dot{\omega}_x(t) &= -\dot{m}\left(\frac{1}{4}r^2+\frac{1}{12}l^2\right)\omega_x(t) - m\left(\frac{1}{4}r^2\right. \\
&\quad \left.+\frac{1}{12}l^2\right)\omega_y(t)\,\omega_z(t) + M_{Int_x}(t) + U_x(t) \\
m(t)\left(\frac{1}{4}r^2+\frac{1}{12}l^2\right)\dot{\omega}_y(t) &= -\dot{m}\left(\frac{1}{4}r^2+\frac{1}{12}l^2\right)\omega_y(t) - m\left(\frac{1}{12}l^2\right. \\
&\quad \left.-\frac{1}{4}r^2\right)\omega_x(t)\,\omega_z(t) + M_{Int_y}(t) + U_y(t) \\
m(t)\left(\frac{1}{2}r^2\right)\dot{\omega}_z(t) &= -\dot{m}\left(\frac{1}{2}r^2\right)\omega_z(t) + M_{Int_z}(t) + U_z(t)
\end{aligned}
\tag{3.13}
$$

The system is linearized by applying the small perturbation method. The small perturbation method is a method in which a variable is assumed to be equivalent to its equilibrium point plus a small perturbation. For example, $\psi(t) = \psi^* + \delta\psi(t)$, where δ denotes some small change in the preceding variable, and * denotes the equilibrium point of that variable.

The equilibrium points for the linearized system are $(\psi^*, \theta^*, \phi^*) = (0,0,0)$, $\dot{\vec{S}}^{B*} = \vec{v}^{B*} = [0,0,-C]^T$ and $\vec{F}^{B*}_{Thrust}(t) = [0,0,-m(t)\,g]^T$, where $F_{Thrust}(t)$ is the thrust of the launch vehicle's engine, and where $-C$ is some constant velocity in the $\hat{k}$ direction. Lastly, the equilibrium point, $\vec{U}^{B*}(t)$ cancels out the internal moments originating from the launch vehicle's engine, and takes the form $\vec{U}^{B*}(t) = \left[-M_{Int_x}(t), -M_{Int_y}(t), -M_{Int_z}(t)\right]^T$. Applying the small perturbation method, and neglecting higher order terms to Eq. (3.7), Eq. (3.11) and Eq. (3.13) yield the linearized equations,

$$
\begin{aligned}
m(t)\,\delta\dot{v}_x(t) &= \delta F_{Thrust_x}(t) - m(t)\,\delta\theta(t)\,g - \dot{m}\delta v_x(t) + m(t)\,\delta\omega_y(t)\,C \\
m(t)\,\delta\dot{v}_y(t) &= \delta F_{Thrust_y}(t) + m(t)\,\delta\psi(t)\,g - \dot{m}\delta v_y(t) - m(t)\,\delta\omega_x(t)\,C \\
m(t)\,\delta\dot{v}_z(t) &= \delta F_{Thrust_z}(t) - \dot{m}\delta v_z(t)
\end{aligned}
\tag{3.14}
$$

$$\begin{aligned}
\delta\dot{S}_x(t) &= \delta v_x(t) \\
\delta\dot{S}_y(t) &= \delta v_y(t) \\
\delta\dot{S}_z(t) &= \delta v_z(t)
\end{aligned} \tag{3.15}$$

$$\begin{aligned}
m(t)\,\delta\dot{\omega}_x(t) &= -\dot{m}\delta\omega_x(t) + \frac{\delta U_x(t)}{\left(\frac{1}{4}r^2 + \frac{1}{12}l^2\right)} \\
m(t)\,\delta\dot{\omega}_y(t) &= -\dot{m}\delta\omega_y(t) + \frac{\delta U_y(t)}{\left(\frac{1}{4}r^2 + \frac{1}{12}l^2\right)} \\
m(t)\,\delta\dot{\omega}_z(t) &= -\dot{m}\delta\omega_z(t) + \frac{\delta U_z(t)}{\left(\frac{1}{2}r^2\right)}
\end{aligned} \tag{3.16}$$

$$\begin{aligned}
\delta\dot{\psi}(t) &= \delta\omega_x(t) \\
\delta\dot{\theta}(t) &= \delta\omega_y(t) \\
\delta\dot{\phi}(t) &= \delta\omega_z(t)
\end{aligned} \tag{3.17}$$

It is worth noting that, since the mass of the launch vehicle, $m(t)$, is a known linear function, Eq. (3.6), where, $\dot{m}$, is the constant slope of the function, no linearization is required for the function $m(t)$. Solving Eq. (3.14) and Eq. (3.16) for $\delta\vec{v}(t)$ and $\delta\vec{\omega}(t)$, respectively, and dropping the δ notation provides the final linearized equations of motion for the launch vehicle,

$$\begin{aligned}
\dot{v}_x(t) &= \frac{F_{Thrust_x}(t)}{m(t)} - \theta(t)\,g - \frac{\dot{m}}{m(t)}v_x(t) + \omega_y(t)\,C \\
\dot{v}_y(t) &= \frac{F_{Thrust_y}(t)}{m(t)} + \psi(t) - \frac{\dot{m}}{m(t)}v_y(t) - \omega_x(t)\,C \\
\dot{v}_z(t) &= \frac{F_{Thrust_z}(t)}{m(t)} - \frac{\dot{m}}{m(t)}v_z(t)
\end{aligned} \tag{3.18}$$

$$\begin{aligned}
\dot{S}_x(t) &= v_x(t) \\
\dot{S}_y(t) &= v_y(t) \\
\dot{S}_z(t) &= v_z(t)
\end{aligned} \tag{3.19}$$

$$\begin{aligned}
\dot{\omega}_x(t) &= -\frac{\dot{m}}{m(t)}\omega_x(t) + \frac{U_x(t)}{m(t)\left(\frac{1}{4}r^2 + \frac{1}{12}l^2\right)} \\
\dot{\omega}_y(t) &= -\frac{\dot{m}}{m(t)}\omega_y(t) + \frac{U_y(t)}{m(t)\left(\frac{1}{4}r^2 + \frac{1}{12}l^2\right)} \\
\dot{\omega}_z(t) &= -\frac{\dot{m}}{m(t)}\omega_z(t) + \frac{U_z(t)}{m(t)\left(\frac{1}{2}r^2\right)}
\end{aligned} \tag{3.20}$$

$$\begin{aligned}
\dot{\psi}(t) &= \omega_x(t) \\
\dot{\theta}(t) &= \omega_y(t) \\
\dot{\phi}(t) &= \omega_z(t)
\end{aligned} \tag{3.21}$$

3.4 Controller Design

In this section, the derivation of the LQR controller is presented and followed by its proof, which utilizes Lyapunov's Direct Method for nonautonomous systems. Next, the derivation and proof of the PD-type controller is presented since the proof of the PD-type controller follows in the same light as the LQR controller proof. The affine-parameter dependent Lyapunov function based controller is then presented, followed by its proof, which also utilizes Lyapunov's Direct Method for nonautonomous systems. Lastly, the derivation of the adaptive controller is presented. Since the adaptive controller is derived using Lyapunov's Direct Method for nonautonomous systems, the derivation doubles as the controller's proof, which also utilizes Barbalat's Lemma.

3.4.1 LQR Controller Derivation

The LQR controller is designed by first representing the linear time-varying system in state-space form,

$$\dot{\vec{x}}(t) = A(t)\vec{x}(t) + B(t)\vec{u}(t)$$

where,

$$\vec{x}(t) = [v_x(t), v_y(t), v_z(t), \omega_x(t), \omega_y(t), \omega_z(t), S_x(t), S_y(t), S_z(t), \psi(t), \theta(t), \phi(t)]^T$$
$$\dot{\vec{x}}(t) = \left[\dot{v}_x(t), \dot{v}_y(t), \dot{v}_z(t), \dot{\omega}_x(t), \dot{\omega}_y(t), \dot{\omega}_z(t), \dot{S}_x(t), \dot{S}_y(t), \dot{S}_z(t), \dot{\psi}(t), \dot{\theta}(t), \dot{\phi}(t)\right]^T$$
$$\vec{u}(t) = \left[F_{Thrust_x}(t), F_{Thrust_y}(t), F_{Thrust_z}(t), U_x(t), U_y(t), U_z(t)\right]^T$$

The resulting $A(t)$ and $B(t)$ matrices are the linearized state and input matrices and are given by,

$$A(t) = \begin{bmatrix}
-\frac{\dot{m}}{m(t)} & 0 & 0 & 0 & C & 0 & 0 & 0 & 0 & 0 & -g & 0 \\
0 & -\frac{\dot{m}}{m(t)} & 0 & -C & 0 & 0 & 0 & 0 & 0 & g & 0 & 0 \\
0 & 0 & -\frac{\dot{m}}{m(t)} & 0 & 0 & 0 & 0 & 0 & 0 & 0 & 0 & 0 \\
0 & 0 & 0 & -\frac{\dot{m}}{m(t)} & 0 & 0 & 0 & 0 & 0 & 0 & 0 & 0 \\
0 & 0 & 0 & 0 & -\frac{\dot{m}}{m(t)} & 0 & 0 & 0 & 0 & 0 & 0 & 0 \\
0 & 0 & 0 & 0 & 0 & -\frac{\dot{m}}{m(t)} & 0 & 0 & 0 & 0 & 0 & 0 \\
1 & 0 & 0 & 0 & 0 & 0 & 0 & 0 & 0 & 0 & 0 & 0 \\
0 & 1 & 0 & 0 & 0 & 0 & 0 & 0 & 0 & 0 & 0 & 0 \\
0 & 0 & 1 & 0 & 0 & 0 & 0 & 0 & 0 & 0 & 0 & 0 \\
0 & 0 & 0 & 1 & 0 & 0 & 0 & 0 & 0 & 0 & 0 & 0 \\
0 & 0 & 0 & 0 & 1 & 0 & 0 & 0 & 0 & 0 & 0 & 0 \\
0 & 0 & 0 & 0 & 0 & 1 & 0 & 0 & 0 & 0 & 0 & 0
\end{bmatrix}$$

$$B(t) = \begin{bmatrix} \frac{1}{m(t)} & 0 & 0 & 0 & 0 & 0 \\ 0 & \frac{1}{m(t)} & 0 & 0 & 0 & 0 \\ 0 & 0 & \frac{1}{m(t)} & 0 & 0 & 0 \\ 0 & 0 & 0 & \frac{1}{m(t)\left(\frac{1}{4}r^2+\frac{1}{12}l^2\right)} & 0 & 0 \\ 0 & 0 & 0 & 0 & \frac{1}{m(t)\left(\frac{1}{4}r^2+\frac{1}{12}l^2\right)} & 0 \\ 0 & 0 & 0 & 0 & 0 & \frac{1}{m(t)\left(\frac{1}{2}r^2\right)} \\ 0 & 0 & 0 & 0 & 0 & 0 \\ 0 & 0 & 0 & 0 & 0 & 0 \\ 0 & 0 & 0 & 0 & 0 & 0 \\ 0 & 0 & 0 & 0 & 0 & 0 \\ 0 & 0 & 0 & 0 & 0 & 0 \\ 0 & 0 & 0 & 0 & 0 & 0 \end{bmatrix}$$

Next, the gain matrix K for the LQR controller is obtained by using the "lqr" function from MATLAB's Control System Toolbox [31]. The cost function of the system,

$$J(\vec{u}(t)) = \int_0^\infty \left(\vec{x}^T(t) Q \vec{x}(t) + \vec{u}^T(t) R \vec{u}(t) + 2\vec{x}^T(t) N \vec{u}(t)\right) dt$$

must be minimized and is subject to the linear time-invariant system dynamics, $\dot{\vec{x}}(t) = A\vec{x}(t) + B\vec{u}(t)$. The system is solved by the Riccati equation

$$A^T S + SA - (SB + N) R^{-1} \left(B^T S + N^T\right) + Q = 0$$

The solution of the Riccati equation, S, is then used to find K in the equation,

$$K = R^{-1} \left(B^T S + N^T\right)$$

The optimal input of the system is then $\vec{u}(t) = -K\vec{x}(t)$. This research sets $A = A_0$ and $B = B_0$, where A_0 and B_0 are the initial states of the $A(t)$ and $B(t)$ matrices, respectively. This provides an optimal gain matrix, K_0, designed about the initial state of the launch vehicle.

3.4.2 LQR Controller Proof

Using the Lyapunov Direct Method for nonautonomous systems, we can choose a candidate Lyapunov function to take the form of the positive definite quadratic function,

$$V(\vec{x}(t), t) = \frac{1}{2}\vec{x}^T(t) P \vec{x}(t) \tag{3.22}$$

where, $P = I^{12\times 12}$. The derivative of the candidate function follows as,

$$\dot{V}(\vec{x}(t), t) = \vec{x}^T(t)\,\dot{\vec{x}}(t)$$

Substituting the closed-loop dynamics of the system, $\dot{\vec{x}}(t) = A_c(t)\,\vec{x}(t)$, yields,

$$\dot{V}(\vec{x}(t), t) = \vec{x}^T(t)\,(A(t) - B(t)\,K_0)\,\vec{x}(t) \tag{3.23}$$

where, $A_c(t) = (A(t) - B(t)\,K_0)$. We can then upper bound $\dot{V}(\vec{x}(t), t)$ with the negative of the positive definite, radially unbounded continuous function, $W(\vec{x}(t)) = -\vec{x}^T(t)\,(A_0 - B_0K_0)\,\vec{x}(t)$,

$$\dot{V}(\vec{x}(t), t) \leq -W(\vec{x}(t))$$

We can prove that $-W(\vec{x}(t))$ provides an upper bound for $\dot{V}(\vec{x}(t), t)$ by examining the behavior of the elements of $A_c(t)$. Starting with the $-B(t)\,K_0$ term, we see that since, $m_0^{-1} \leq m^{-1}(t)\ \forall\ t_f \geq t \geq 0$, it is trivial that $[B_0K_0]_{i,j} \leq [B(t)\,K_0]_{i,j}\ \forall\ t_f \geq t \geq 0$, for $i = 1, ..., 12$ and $j = 1, ..., 6$. Here, $[B_0K_0]_{i,j}$ denotes the i^{th}, j^{th} component of the enclosed matrix, B_0K_0. Next, we examine the first six diagonal elements of $A_c(t)$, since these elements correspond to the only time-dependent elements of $A(t)$. We can write these elements of

$A_c\,(t)$ as,

$$\begin{bmatrix} A_{c_{1,1}}(t) \\ A_{c_{2,2}}(t) \\ A_{c_{3,3}}(t) \\ A_{c_{4,4}}(t) \\ A_{c_{5,5}}(t) \\ A_{c_{6,6}}(t) \end{bmatrix} = \begin{bmatrix} -\frac{\dot{m}}{m(t)} - \frac{K_{1,1}}{m(t)} \\ -\frac{\dot{m}}{m(t)} - \frac{K_{2,2}}{m(t)} \\ -\frac{\dot{m}}{m(t)} - \frac{K_{3,3}}{m(t)} \\ -\frac{\dot{m}}{m(t)} - \frac{K_{4,4}}{m(t)\left(\frac{1}{4}r^2+\frac{1}{12}l^2\right)} \\ -\frac{\dot{m}}{m(t)} - \frac{K_{5,5}}{m(t)\left(\frac{1}{4}r^2+\frac{1}{12}l^2\right)} \\ -\frac{\dot{m}}{m(t)} - \frac{K_{6,6}}{m(t)\left(\frac{1}{2}r^2\right)} \end{bmatrix} = \frac{1}{m\,(t)} \begin{bmatrix} -\dot{m} - K_{1,1} \\ -\dot{m} - K_{2,2} \\ -\dot{m} - K_{3,3} \\ -\dot{m} - \frac{K_{4,4}}{\left(\frac{1}{4}r^2+\frac{1}{12}l^2\right)} \\ -\dot{m} - \frac{K_{5,5}}{\left(\frac{1}{4}r^2+\frac{1}{12}l^2\right)} \\ -\dot{m} - \frac{K_{6,6}}{\left(\frac{1}{2}r^2\right)} \end{bmatrix}$$

Here, we see that $[A_{c_0}]_{i,j} \leq [A_c(t)]_{i,j}\ \forall\, t_f \geq t \geq 0$, for $i = j = 1, ..., 6$ where, $A_{c_0} = A_0 - B_0 K_0$. We can now confidently state that,

$$\|A_{c_0}\|_2 \leq \|A_c(t)\|_2 \quad \forall \quad t_f \geq t \geq 0 \tag{3.24}$$

where, $\|A_{c_0}\|_2$ denotes the matrix 2-norm of the enclosed matrix, A_{c_0}. The matrix 2-norm assigns a notion of size to an $n \times m$ matrix, which is accomplished by finding the maximum of all possible non-zero vectors of the vector 2-norm of $A_{c_0}\vec{\mathcal{X}}$ divided by the vector 2-norm of the arbitrary vector $\vec{\mathcal{X}}$ [32],

$$\|A_{c_0}\|_2 = \max_{\vec{\mathcal{X}} \neq 0} \frac{\left\|A_{c_0}\vec{\mathcal{X}}\right\|_2}{\left\|\vec{\mathcal{X}}\right\|_2}$$

Essentially, this process provides us with a quantity of how much matrix A_{c_0} expands vector $\vec{\mathcal{X}}$ [32]. Therefore, the matrix 2-norm is useful for comparing the magnitude of two matrices.

We can prove that the inequality defined by Eq. (3.24) holds true for our system by plotting $\|A_c(t)\|_2$ verses time, which is presented in Figure 3.4.

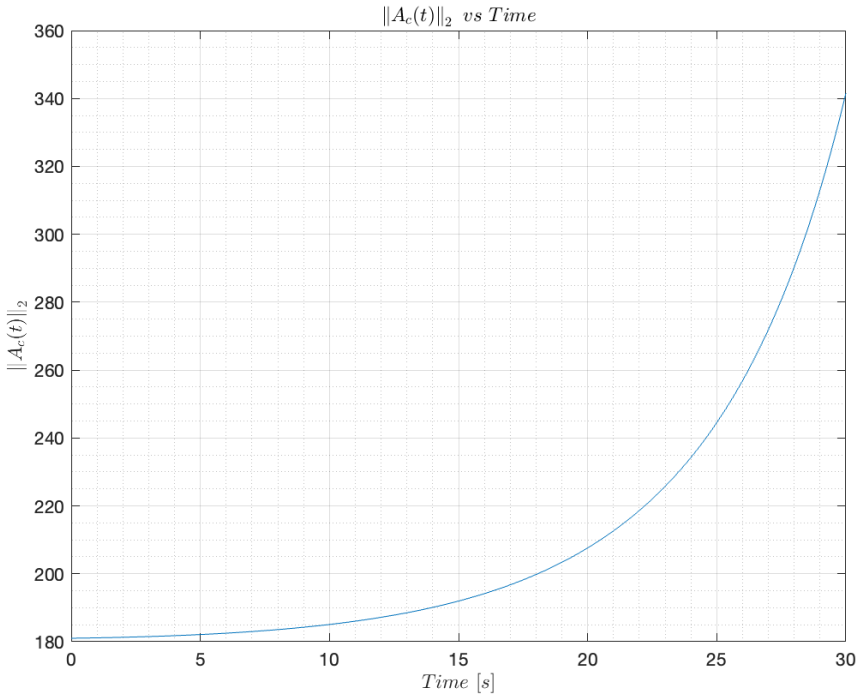

Figure 3.4 $\|A_c(t)\|_2$ vs Time for LQR Controller

From Figure 3.4 we can conclude that Eq. (3.24) holds true since $\|A_c(t)\|_2$ is increasing $\forall\ t_f \geq t \geq 0$. Finally, due to the fact that the gain designed by the LQR function within MATLAB is guaranteed to make the closed-loop dynamics of the initial closed-loop system, A_{c_0}, Hurwitz, and therefore negative definite [33], we may now write the inequality which bounds the derivative of the Lyapunov function more formally as,

$$\vec{x}^T(t)\left(A(t) - B(t)K_0\right)\vec{x}(t) \leq \vec{x}^T(t)\left(A_0 - B_0K_0\right)\vec{x}(t) \leq 0 \quad \forall\ \ \vec{x}(t) \in \mathbb{R}^n, t_f \geq t \geq 0 \tag{3.25}$$

Then, since a positive definite quadratic Lyapunov function is always positive definite decrescent [28], the system is shown to be uniformly asymptotically stable.

3.4.3 PD-Type Controller Derivation

The PD-type controller is designed by considering the obtained linear system as the sum of two subsystems, rotation and translation, denoted by the subscripts, r and t, respectively.

The state and input vectors for each subsystem are $\vec{x}_{r_1}(t) = [\psi(t), \theta(t), \phi(t)]^T$, $\vec{x}_{r_2}(t) = [\omega_x(t), \omega_y(t), \omega_z(t)]^T$, $\vec{u}_r(t) = [U_x(t), U_y(t), U_z(t)]^T$ and $\vec{x}_{t_1}(t) = [S_x(t), S_y(t), S_z(t)]^T$, $\vec{x}_{t_2}(t) = [v_x(t), v_y(t), v_z(t)]^T$, $\vec{u}_t(t) = \left[F_{Thrust_x}(t), F_{Thrust_y}(t), F_{Thrust_z}(t)\right]^T$. The $A_r(t)$ and $B_r(t)$ matrices of the rotational subsystem are,

$$A_r(t) = \begin{bmatrix} -\frac{\dot{m}}{m(t)} & 0 & 0 \\ 0 & -\frac{\dot{m}}{m(t)} & 0 \\ 0 & 0 & -\frac{\dot{m}}{m(t)} \end{bmatrix}$$

$$B_r(t) = \begin{bmatrix} \frac{1}{m(t)\left(\frac{1}{4}r^2+\frac{1}{12}l^2\right)} & 0 & 0 \\ 0 & \frac{1}{m(t)\left(\frac{1}{4}r^2+\frac{1}{12}l^2\right)} & 0 \\ 0 & 0 & \frac{1}{m(t)\left(\frac{1}{2}r^2\right)} \end{bmatrix}$$

The subsystem's linear dynamics are,

$$\begin{aligned} \dot{\vec{x}}_{r_1}(t) &= \vec{x}_{r_2}(t) \\ \dot{\vec{x}}_{r_2}(t) &= A_r(t)\,\vec{x}_{r_2}(t) + B_r(t)\,\vec{u}_r(t) \end{aligned} \tag{3.26}$$

For the PD-type controller, the P-gain is arbitrarily set to 1, and the D-gain, k_r, must be greater than zero. The error vector is defined as,

$$\vec{e}_r(t) = \vec{x}_{r_1}(t) + k_r\vec{x}_{r_2}(t)$$

whose derivative follows as,

$$\dot{\vec{e}}_r(t) = \dot{\vec{x}}_{r_1}(t) + k_r\dot{\vec{x}}_{r_2}(t) = \vec{x}_{r_2}(t) + k_r\left(A_r(t)\,\vec{x}_{r_2}(t) + B_r(t)\,\vec{u}_r(t)\right) \tag{3.27}$$

The control input can then be written as,

$$\vec{u}_r(t) = B_r^{-1}(t)\left[-A_r(t)\,\vec{x}_{r_2}(t) - \vec{x}_{r_2}(t) - \frac{1}{k_r}\left(\vec{x}_{r_2}(t) + \vec{x}_{r_1}(t)\right)\right] \tag{3.28}$$

Plugging this into Eq. (3.27) yields,

$$\dot{\vec{e}}_r(t) = \vec{x}_{r_1}(t) + k_r\left[A_r(t)\,\vec{x}_{r_2}(t) - A_r(t)\,\vec{x}_{r_2}(t) - \vec{x}_{r_2}(t) - \frac{1}{k_r}\left(\vec{x}_{r_2}(t) + \vec{x}_{r_1}(t)\right)\right]$$

When this equation is simplified, it is shown that $\vec{e}_r(t)$ converges to zero exponentially, proving that Eq. (3.28) is a correct form of the control input for the linearized subsystem model,

$$\dot{\vec{e}}_r(t) = -k_r\vec{x}_{r_2}(t) - \vec{x}_{r_1}(t) = -\vec{e}_r(t)$$

Similarly, the derivation for the PD-type control of the rotational subsystem begins with the A_t and B_t matrices corresponding to the subsystem's linear dynamics,

$$A_t(t) = A_r(t)$$

$$B_t(t) = \frac{1}{m(t)}$$

$$\dot{\vec{x}}_{t_1}(t) = \vec{x}_{t_2}(t)$$

$$\dot{\vec{x}}_{t_2}(t) = A_t(t)\,\vec{x}_{t_2}(t) + B_t(t)\,\vec{u}_t(t)$$

The error of the PD-controlled system is then defined as,

$$\vec{e}_t(t) = \vec{x}_{t_1}(t) + k_t\vec{x}_{t_2}(t)$$

Once again, the P-gain is set to 1, and the D-gain, k_t, must be greater than zero. The derivative of the error vector then takes the form,

$$\dot{\vec{e}}_t(t) = \dot{\vec{x}}_{t_1}(t) + k_t \dot{\vec{x}}_{t_2}(t) = \vec{x}_{t_2}(t) + k_t \left(A_t(t) \vec{x}_{t_2}(t) + F(t) + B_t(t) \vec{u}_t(t) \right) \tag{3.29}$$

Since the translational equation of motion is coupled to the rotational equation of motion, the vector $F(t)$ is employed to provide the following relation,

$$F(t) = \begin{bmatrix} 0 & -g & 0 \\ g & 0 & 0 \\ 0 & 0 & 0 \end{bmatrix} \vec{x}_{r_1}(t) + \begin{bmatrix} 0 & C & 0 \\ -C & 0 & 0 \\ 0 & 0 & 0 \end{bmatrix} \vec{x}_{r_2}(t)$$

The control input for the subsystem, $\vec{u}_t(t)$, is then defined as,

$$\vec{u}_t(t) = B_t^{-1}(t) \left[-A_t(t) \vec{x}_{t_2}(t) - F(t) - \vec{x}_{t_2}(t) - \frac{1}{k_t} \left(\vec{x}_{t_1}(t) + \vec{x}_{t_2}(t) \right) \right]$$

This equation is substituted into the derivative of the error, Eq. (3.29), and yields,

$$\dot{\vec{e}}_t(t) = \vec{x}_{t_2}(t) + k_t \left[A_t(t) \vec{x}_{t_2}(t) + F(t) - A_t(t) \vec{x}_{t_2}(t) - F(t) - \vec{x}_{t_2}(t) - \frac{1}{k_t} \left(\vec{x}_{t_1}(t) + \vec{x}_{t_2}(t) \right) \right]$$

When simplified, it is shown that the derived control input, $\vec{u}_t(t)$, makes the error converge to zero exponentially,

$$\dot{\vec{e}}_t(t) = -k_t \vec{x}_{t_2}(t) - \vec{x}_{t_1}(t) = -\vec{e}_t(t)$$

In the same light as the LQR controller, the matrices $A_r(t)$, $B_r(t)$, $A_t(t)$, $B_t(t)$, and $F(t)$ are set to their initial values, A_{r_0}, B_{r_0}, A_{t_0}, B_{t_0}, and F_0, respectively.

3.4.4 PD-Type Controller Proof

The proof of the PD-type controller is the same as the proof for the LQR controller, since the PD-type controller may also generate a stabilizing gain, K_0, such that the initial

closed-loop system, A_{c_0}, is Hurwitz. For this controller, K_0 will take the form,

$$K_0 = -B_{t_0}^{-1} \begin{bmatrix} A_{t_0} + \left(1 + \frac{1}{k_t}\right) I^{3\times 3} & \begin{bmatrix} 0 & C & 0 \\ -C & 0 & 0 \\ 0 & 0 & 0 \end{bmatrix} & \frac{1}{k_t} I^{3\times 3} & \begin{bmatrix} 0 & -g & 0 \\ g & 0 & 0 \\ 0 & 0 & 0 \end{bmatrix} \\ 0 & A_{r_0} + \left(1 + \frac{1}{k_r}\right) I^{3\times 3} & 0 & \frac{1}{k_r} I^{3\times 3} \end{bmatrix}$$

In the same fashion as the proof for the LQR controller, we can prove that Eq. (3.24) holds for this system by plotting $\|A_c(t)\|_2$ verses time, which is presented in Figure 3.5.

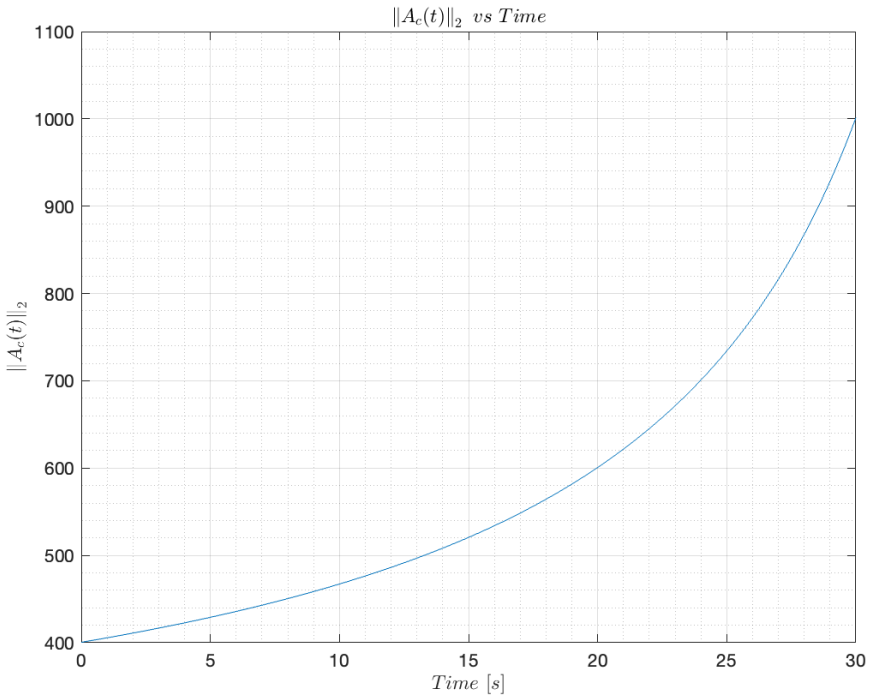

Figure 3.5 $\|A_c(t)\|_2$ vs Time for PD-Type Controller

From Figure 3.5 we can conclude that Eq. (3.24) holds true for this system since $\|A_c(t)\|_2$ is increasing $\forall\ t_f \geq t \geq 0$. Therefore, the system is shown to be uniformly asymptotically stable since a Lyapunov function for this system may be chosen to be equal to Eq. (3.22), whose derivative is defined by Eq. (3.23), which is bounded by the inequality defined in Eq. (3.25).

3.4.5 Affine-Parameter Dependent Lyapunov Function Based Controller

Linear Parameter-Varying (LPV) Lyapunov approaches are distinctly different than conventional gain-scheduling approaches since they derive a controller directly, instead of through the derivation of a combination of multiple linear time-invariant controllers [26]. The affine quadratic Lyapunov function state feedback controller background is presented in Bara et al. and Gahinet et al. [27, 34], which state that given a generalized LPV system,

$$\dot{\vec{x}}(t) = A\left(\vec{\sigma}\left(t\right)\right)\vec{x}(t) + B\left(\vec{\sigma}\left(t\right)\right)\vec{u}(t) \tag{3.30}$$

where $\vec{x}(t) \in \mathbb{R}^n$ is the state vector, and $\vec{x}\left(0\right) = \vec{x}_0$, in which the state and input matrices, $A\left(\vec{\sigma}\left(t\right)\right)$ and $B\left(\vec{\sigma}\left(t\right)\right)$, depend affinely on the time-varying parameter vector, $\vec{\sigma}\left(t\right)$ with the form,

$$\begin{aligned} A\left(\vec{\sigma}\left(t\right)\right) &= A_0 + \textstyle\sum_{i=1}^{i=N} \sigma_i\left(t\right) A_i \\ B\left(\vec{\sigma}\left(t\right)\right) &= B_0 + \textstyle\sum_{i=1}^{i=N} \sigma_i\left(t\right) B_i \end{aligned} \tag{3.31}$$

Here, $\vec{\sigma}\left(t\right) = \left[\ \sigma_1\left(t\right) \quad ... \quad \sigma_N\left(t\right)\ \right]^T \in \mathbb{R}^N$ is the time-varying parameter vector that satisfies the following constraints,

$$\begin{aligned} \sigma_i\left(t\right) &\in \left[\ \underline{\sigma_i} \quad \overline{\sigma_i}\ \right] \\ \dot{\sigma}_i\left(t\right) &\in \left[\ \underline{\dot{\sigma}_i} \quad \overline{\dot{\sigma}_i}\ \right] \end{aligned} \tag{3.32}$$

Each element of the time-varying parameter vector, $\sigma_i\left(t\right)$, ranges between the known lower and upper bounds, $\underline{\sigma_i}$ and $\overline{\sigma_i}$. Similarly, the time-varying rate of variation of $\sigma_i\left(t\right)$, denoted by $\dot{\sigma}_i\left(t\right)$ ranges between the known lower and upper bounds, $\underline{\dot{\sigma}_i}$ and $\overline{\dot{\sigma}_i}$. These assumptions establish the parameter vector and the rate of variation of the parameter vector, $\dot{\vec{\sigma}}\left(t\right)$, be to

valued in hyper rectangles with vertices defined by,

$$\Gamma = \left\{ \begin{pmatrix} \gamma_1 & ... & \gamma_N \end{pmatrix} : \gamma \in \begin{Bmatrix} \underline{\sigma_i} & \overline{\sigma_i} \end{Bmatrix} \right\}$$
$$\Lambda = \left\{ \begin{pmatrix} \lambda_1 & ... & \lambda_N \end{pmatrix} : \lambda \in \begin{Bmatrix} \underline{\dot{\sigma}_i} & \overline{\dot{\sigma}_i} \end{Bmatrix} \right\} \tag{3.33}$$

This research selects the variational parameter to be equivalent to the inverse of the launch vehicle's mass, $\vec{\sigma}(t) = m(t)^{-1}$. The rate of variation of the variational parameter then follows as $\dot{\vec{\sigma}}(t) = -m(t)^{-2}\dot{m}$ since $m(t)$ abides by Eq. (3.1).

Affine Quadratic Stability

From Bara et al. and Gahinet et al. [27, 34], the LPV system is said to be affinely quadratically stable (AQS) if there exists an affine quadratic Lyapunov function,

$$V(\vec{x}(t), \vec{\sigma}(t)) = \vec{x}^T(t) P(\vec{\sigma}(t)) \vec{x}(t) \tag{3.34}$$

such that $V(\vec{x}(t), \vec{\sigma}(t)) > 0$ and $\dot{V}\left(\vec{x}(t), \vec{\sigma}(t), \dot{\vec{\sigma}}(t)\right) < 0$ for all admissible parameter trajectories and all initial conditions x_0, where $P(\vec{\sigma}(t))$ is a symmetric Lyapunov matrix affine in $\vec{\sigma}(t)$, and defined by,

$$P(\vec{\sigma}(t)) = P_0 + \sum_{i=1}^{i=N} \sigma_i(t) P_i \tag{3.35}$$

If $\sigma_i(t)$ and $\dot{\sigma}_i(t)$ abide by Eq. (3.33), then the asymptotic stability of the system is guaranteed by standard Lyapunov theory. AQS is less conservative than standard quadratic stability since AQS incorporates the rate of parameter variation, while standard quadratic stability neglects this [27, 34].

Feedback Controller

From Bara et al. [27], the state-feedback controller will take the form of,

$$\vec{u}(t) = K\left(\vec{\sigma}\left(t\right)\right)\vec{x}(t) \tag{3.36}$$

where the state-feedback gain matrix, $K\left(\vec{\sigma}\left(t\right)\right)$, is affine in $\vec{\sigma}\left(t\right)$, and defined by,

$$K\left(\vec{\sigma}\left(t\right)\right) = K_0 + \sum_{i=1}^{i=N} \sigma_i\left(t\right) K_i \tag{3.37}$$

If there exists matrices, G, L, symmetric matrices, P_0^{-1}, P_1^{-1}, ..., P_N^{-1}, and positive scalars, τ_1, ..., τ_N such that the linear matrix inequalities,

$$\begin{bmatrix} -\left(G+G\right) & GA^T\left(\gamma\right) + L\mathcal{E}^T\left(\gamma\right) + P^{-1}\left(\gamma\right) & G \\ A\left(\gamma\right)G + \mathcal{E}\left(\gamma\right)L + P^{-1}\left(\gamma\right) & -P^{-1}\left(\gamma\right) - P^{-1}\left(\lambda\right) + P_0^{-1} & 0 \\ G & 0 & -P^{-1}\left(\gamma\right) \end{bmatrix} + \sum_i \tau_i \gamma_i^2 \begin{bmatrix} 0 & 0 & 0 \\ 0 & I & 0 \\ 0 & 0 & 0 \end{bmatrix} < 0 \quad \forall \quad (\gamma, \lambda) \in \Gamma \times \Lambda \tag{3.38}$$

and

$$\begin{bmatrix} -\left(G+G\right) & 0 & -P^{-1}\left(\gamma\right) + L\Upsilon_i^T B_i^T & -G \\ 0 & -\left(G+G\right) & -P_1^{-1} + GA_i^T + L\mathcal{H}_i^T\left(\gamma\right) & 0 \\ -P^{-1}\left(\gamma\right) + B_i\Upsilon_i L & -P_i^{-1} + A_i G + \mathcal{H}_i\left(\gamma\right)L & -P^{-1}\left(\gamma\right) - \tau_i I & 0 \\ -G & 0 & 0 & -P^{-1}\left(\gamma\right) \end{bmatrix} \leq 0 \quad \forall \quad \gamma \in \Gamma \tag{3.39}$$

are feasible for $i = 1, ..., N$, where $\Upsilon_i = [0, I, 0]$[1], $\mathcal{E}(\vec{\sigma}(t)) = B(\vec{\sigma}(t))\mathcal{T}(\vec{\sigma}(t))$, $\mathcal{H}_i(\vec{\sigma}(t)) = B(\vec{\sigma}(t))\Upsilon_i + B_i\mathcal{T}(\vec{\sigma}(t))$, and $\mathcal{T}(\vec{\sigma}(t)) = [I, \sigma_1(t) I, ..., \sigma_N(t)]$ then the control law ensures the closed-loop system to be AQS. Lastly, the terms of $K(\vec{\sigma}(t))$ are found by $K_i = L_i G$ with $L = [L_0^T, L_1^T, ..., L_N^T]^T$.

3.4.6 Affine-Parameter Dependent Lyapunov Function Based Controller Proof

From Bara et al. [27], substituting the state-feedback control law into the generalized LPV system yields,

$$\dot{\vec{x}}(t) = A(\vec{\sigma}(t))\vec{x}(t) + B(\vec{\sigma}(t))K(\vec{\sigma}(t))\vec{x}(t) \tag{3.40}$$

which may be simplified to,

$$\dot{\vec{x}}(t) = \widetilde{A}(\vec{\sigma}(t))\vec{x}(t) \tag{3.41}$$

where $\widetilde{A}(\vec{\sigma}(t)) = A(\vec{\sigma}(t)) + B(\vec{\sigma}(t))K(\vec{\sigma}(t))$. By substituting the state-feedback control law into the affine quadratic Lyapunov function, the previously stated AQS theory may be reformulated,

$$\begin{aligned}\dot{V}\left(\vec{x}(t), \vec{\sigma}(t), \dot{\vec{\sigma}}(t)\right) = {} & \vec{x}^T(t) A(\vec{\sigma}(t))^T P(\vec{\sigma}(t))\vec{x}(t) + \vec{x}^T(t) P(\vec{\sigma}(t)) A(\vec{\sigma}(t))\vec{x}(t) \\ & + \vec{x}^T(t)\frac{dP(\vec{\sigma}(t))}{dt}\vec{x}(t)\end{aligned} \tag{3.42}$$

From Eq. (3.34) it is found that $dP(\vec{\sigma}(t))/dt = P\left(\dot{\vec{\sigma}}(t)\right) - P_0$,

$$\begin{aligned}\dot{V}\left(\vec{x}(t), \vec{\sigma}(t), \dot{\vec{\sigma}}(t)\right) = \vec{x}^T(t)\Big[& A(\vec{\sigma}(t))^T P(\vec{\sigma}(t)) + P(\vec{\sigma}(t)) A(\vec{\sigma}(t)) \\ & + P\left(\dot{\vec{\sigma}}(t)\right) - P_0\Big]\vec{x}(t)\end{aligned} \tag{3.43}$$

Using this simplified affine quadratic Lyapunov function, it may be stated that the LPV system is AQS if there exists $N + 1$ symmetric matrices $P_0, ..., P_N$ such that $P(\vec{\sigma}(t)) > 0$

[1] I, is located in the $i + 1$ block

and,

$$A\left(\vec{\sigma}\left(t\right)\right)^{T}P\left(\vec{\sigma}\left(t\right)\right)+P\left(\vec{\sigma}\left(t\right)\right)A\left(\vec{\sigma}\left(t\right)\right)+P\left(\dot{\vec{\sigma}}\left(t\right)\right)-P_{0}<0\quad\forall\quad\vec{x}(t)\neq0 \tag{3.44}$$

The dual of the Lyapunov LMI, Eq. (3.44), may be found by multiplying both sides of the LMI by $P^{-1}\left(\vec{\sigma}\left(t\right)\right)$,

$$\begin{aligned}P^{-1}\left(\vec{\sigma}\left(t\right)\right)A\left(\vec{\sigma}\left(t\right)\right)^{T}+A\left(\vec{\sigma}\left(t\right)\right)P^{-1}\left(\vec{\sigma}\left(t\right)\right)+P^{-1}\left(\vec{\sigma}\left(t\right)\right)P\left(\dot{\vec{\sigma}}\left(t\right)\right)P^{-1}\left(\vec{\sigma}\left(t\right)\right)\\-P^{-1}\left(\vec{\sigma}\left(t\right)\right)P_{0}P^{-1}\left(\vec{\sigma}\left(t\right)\right)<0\end{aligned} \tag{3.45}$$

Since $P\left(\vec{\sigma}\left(t\right)\right)$ is a positive symmetric matrix it may be stated that,

$$P\left(\dot{\vec{\sigma}}\left(t\right)\right)P^{-1}\left(\vec{\sigma}\left(t\right)\right)=-P\left(\vec{\sigma}\left(t\right)\right)P^{-1}\left(\dot{\vec{\sigma}}\left(t\right)\right)$$

Solving for $P^{-1}\left(\dot{\vec{\sigma}}\left(t\right)\right)$ yields,

$$-P^{-1}\left(\dot{\vec{\sigma}}\left(t\right)\right)=P^{-1}\left(\vec{\sigma}\left(t\right)\right)P\left(\dot{\vec{\sigma}}\left(t\right)\right)P^{-1}\left(\vec{\sigma}\left(t\right)\right)$$

Following a similar argument for $P^{-1}\left(\vec{\sigma}\left(t\right)\right)$ and P_{0}^{-1}, we arrive at the dual Lyapunov LMI,

$$P^{-1}\left(\vec{\sigma}\left(t\right)\right)\widetilde{A}\left(\vec{\sigma}\left(t\right)\right)+\widetilde{A}\left(\vec{\sigma}\left(t\right)\right)P^{-1}\left(\vec{\sigma}\left(t\right)\right)-P^{-1}\left(\dot{\vec{\sigma}}\left(t\right)\right)+P_{0}^{-1}<0 \tag{3.46}$$

The dual Lyapunov LMI is now bounded by the multiconvex function, $\mathcal{V}_{convex}\left(\vec{x}(t),\vec{\sigma}\left(t\right),\dot{\vec{\sigma}}\left(t\right)\right)$ (multiconvexity meaning convexity along each direction $\sigma_{i}\left(t\right)$ of the parameter space [34]),

$$\mathcal{V}_{convex}\left(\vec{x}(t),\vec{\sigma}\left(t\right),\dot{\vec{\sigma}}\left(t\right)\right)=\mathcal{V}\left(\vec{x}(t),\vec{\sigma}\left(t\right),\dot{\vec{\sigma}}\left(t\right)\right)+\vec{x}^{T}(t)\sum_{i}\tau_{i}\sigma_{i}^{2}\left(t\right)I_{n}\vec{x}(t) \tag{3.47}$$

where,

$$\mathcal{V}\left(\vec{x}(t),\vec{\sigma}\left(t\right),\dot{\vec{\sigma}}\left(t\right)\right)=\vec{x}^{T}(t)\left[P^{-1}\left(\vec{\sigma}\left(t\right)\right)\widetilde{A}\left(\vec{\sigma}\left(t\right)\right)+\widetilde{A}\left(\vec{\sigma}\left(t\right)\right)P^{-1}\left(\vec{\sigma}\left(t\right)\right)\right.$$
$$\left.-P^{-1}\left(\dot{\vec{\sigma}}\left(t\right)\right)+P_{0}^{-1}\right]\vec{x}(t) \tag{3.48}$$

and $\tau_i > 0$. Since $\mathcal{V}_{convex}\left(\vec{x}(t),\vec{\sigma}\left(t\right),\dot{\vec{\sigma}}\left(t\right)\right) \geq \mathcal{V}\left(\vec{x}(t),\vec{\sigma}\left(t\right),\dot{\vec{\sigma}}\left(t\right)\right)$, it may now be stated that the generalized LPV system satisfies the AQS conditions if $\mathcal{V}_{convex}\left(\vec{x}(t),\vec{\sigma}\left(t\right),\dot{\vec{\sigma}}\left(t\right)\right) < 0$ and $P^{-1}\left(\vec{\sigma}\left(t\right)\right) > 0 \;\forall\; \vec{x}(t) \neq 0$ are satisfied for all admissible parameter trajectories.

The feasibility LMI, Eq. (3.48), is now studied. Considering $K_i G = L_i$, it may be shown that $\mathcal{E}\left(\gamma\right)L = \mathcal{E}\left(\gamma\right)K\left(\gamma\right)G$, which when substituted into Eq. (3.38) yields,

$$\begin{bmatrix} -\left(G+G\right) & GA^{T}\left(\gamma\right)+\left(\mathcal{E}\left(\gamma\right)K\left(\gamma\right)G\right)^{T}+P^{-1}\left(\gamma\right) & G \\ A\left(\gamma\right)G+\mathcal{E}\left(\gamma\right)K\left(\gamma\right)G+P^{-1}\left(\gamma\right) & -P^{-1}\left(\gamma\right)-P^{-1}\left(\lambda\right)+P_{0}^{-1} & 0 \\ G & 0 & -P^{-1}\left(\gamma\right) \end{bmatrix}$$
$$+\sum_{i}\tau_{i}\gamma_{i}^{2}\begin{bmatrix} 0 & 0 & 0 \\ 0 & I & 0 \\ 0 & 0 & 0 \end{bmatrix} < 0 \quad \forall \quad (\gamma,\lambda)\in\Gamma\times\Lambda \tag{3.49}$$

which simplifies to,

$$\begin{bmatrix} -\left(G+G\right) & G\widetilde{A}\left(\gamma\right)+P^{-1}\left(\gamma\right) & G \\ \widetilde{A}\left(\gamma\right)G+P^{-1}\left(\gamma\right) & -P^{-1}\left(\gamma\right)-P^{-1}\left(\lambda\right)+P_{0}^{-1} & 0 \\ G & 0 & -P^{-1}\left(\gamma\right) \end{bmatrix}$$
$$+\sum_{i}\tau_{i}\gamma_{i}^{2}\begin{bmatrix} 0 & 0 & 0 \\ 0 & I & 0 \\ 0 & 0 & 0 \end{bmatrix}(0,I,0) < 0 \quad \forall \quad (\gamma,\lambda)\in\Gamma\times\Lambda \tag{3.50}$$

and is equivalent to,

$$\begin{bmatrix} 0 & P^{-1}(\gamma) & 0 \\ P^{-1}(\gamma) & -P^{-1}(\gamma) - P^{-1}(\lambda) + P_0^{-1} + \sum_i \tau_i \gamma_i^2 I & 0 \\ 0 & 0 & -P^{-1}(\gamma) \end{bmatrix} + \begin{bmatrix} -I \\ \widetilde{A}(\gamma) \\ I \end{bmatrix} G \begin{bmatrix} I & 0 & 0 \end{bmatrix} + \begin{bmatrix} I \\ 0 \\ 0 \end{bmatrix} G \begin{bmatrix} -I & \widetilde{A}(\gamma) & I \end{bmatrix} < 0 \quad \forall \quad (\gamma, \lambda) \in \Gamma \times \Lambda \tag{3.51}$$

The projection lemma [35] is now used to further simplify the LMI. The right orthogonal complements of $[I, 0, 0]$ and $[-I, \widetilde{A}(\gamma), I]$ are, $\begin{bmatrix} 0 & 0 \\ I & 0 \\ 0 & I \end{bmatrix}$ and $\begin{bmatrix} \widetilde{A}(\gamma) & I \\ I & 0 \\ 0 & I \end{bmatrix}$, respectively. By the projection lemma, the inequality Eq. (3.51) may be re-written as two inequalities,

$$\begin{bmatrix} 0 & 0 \\ I & 0 \\ 0 & I \end{bmatrix}^T \begin{bmatrix} 0 & P^{-1}(\gamma) & 0 \\ P^{-1}(\gamma) & -P^{-1}(\gamma) - P^{-1}(\lambda) + P_0^{-1} + \sum_i \tau_i \gamma_i^2 I & 0 \\ 0 & 0 & -P^{-1}(\gamma) \end{bmatrix} \begin{bmatrix} 0 & 0 \\ I & 0 \\ 0 & I \end{bmatrix} < 0 \quad \forall \quad (\gamma, \lambda) \in \Gamma \times \Lambda \tag{3.52}$$

$$\begin{bmatrix} \widetilde{A}(\gamma) & I \\ I & 0 \\ 0 & I \end{bmatrix}^T \begin{bmatrix} 0 & P^{-1}(\gamma) & 0 \\ P^{-1}(\gamma) & -P^{-1}(\gamma) - P^{-1}(\lambda) + P_0^{-1} + \sum_i \tau_i \gamma_i^2 I & 0 \\ 0 & 0 & -P^{-1}(\gamma) \end{bmatrix} \begin{bmatrix} \widetilde{A}(\gamma) & I \\ I & 0 \\ 0 & I \end{bmatrix} < 0 \quad \forall \quad (\gamma, \lambda) \in \Gamma \times \Lambda \tag{3.53}$$

Simplifying these inequalities yields,

$$\begin{bmatrix} -P^{-1}(\gamma) - P^{-1}(\lambda) + P_0^{-1} + \sum_i \tau_i \gamma_i^2 I & 0 \\ 0 & -P^{-1}(\gamma) \end{bmatrix} < 0 \quad \forall \quad (\gamma, \lambda) \in \Gamma \times \Lambda \tag{3.54}$$

$$\begin{bmatrix} -P^{-1}(\gamma) + P^{-1}(\gamma)\widetilde{A}(\gamma) + \widetilde{A}(\gamma)P^{-1}(\gamma) - P^{-1}(\lambda) + P_0^{-1} + \sum_i \tau_i \gamma_i^2 I & P^{-1}(\gamma) \\ P^{-1}(\gamma) & -P^{-1}(\gamma) \end{bmatrix} < 0 \quad \forall \quad (\gamma, \lambda) \in \Gamma \times \Lambda \tag{3.55}$$

Next, the inequalities are further simplified by the Schur Complement [36], which generates the four inequalities,

$$-P^{-1}(\gamma) - P^{-1}(\lambda) + P_0^{-1} + \sum_i \tau_i \gamma_i^2 I < 0 \quad \forall \quad (\gamma, \lambda) \in \Gamma \times \Lambda \tag{3.56}$$

$$P^{-1}(\gamma) > 0 \quad \forall \quad \gamma \in \Gamma \tag{3.57}$$

$$-P^{-1}(\gamma) + P^{-1}(\gamma)\widetilde{A}(\gamma) + \widetilde{A}(\gamma)P^{-1}(\gamma) - P^{-1}(\lambda) + P_0^{-1} + \sum_i \tau_i \gamma_i^2 I < 0 \quad \forall \quad (\gamma, \lambda) \in \Gamma \times \Lambda \tag{3.58}$$

$$-P^{-1}(\gamma) - P^{-1}(\gamma)\left(-P^{-1}(\gamma) + P^{-1}(\gamma)\widetilde{A}(\gamma) + \widetilde{A}(\gamma)P^{-1}(\gamma) - P^{-1}(\lambda) + P_0^{-1} + \sum_i \tau_i \gamma_i^2 I\right)^{-1} P^{-1}(\gamma) < 0 \quad \forall \quad (\gamma, \lambda) \in \Gamma \times \Lambda \tag{3.59}$$

The inequalities Eq. (3.58) and Eq. (3.59) are both feasible if

$$P^{-1}(\gamma)\widetilde{A}(\gamma) + \widetilde{A}(\gamma)P^{-1}(\gamma) - P^{-1}(\lambda) + P_0^{-1} + \sum_i \tau_i \gamma_i^2 I < 0 \quad \forall \quad (\gamma, \lambda) \in \Gamma \times \Lambda \tag{3.60}$$

is feasible. This simplifies the four inequalities into the three final inequalities,

$$-P^{-1}(\gamma) - P^{-1}(\lambda) + P_0^{-1} + \textstyle\sum_i \tau_i \gamma_i^2 I < 0 \quad \forall \quad (\gamma, \lambda) \in \Gamma \times \Lambda \tag{3.61}$$

$$P^{-1}(\gamma) > 0 \quad \forall \quad \gamma \in \Gamma \tag{3.62}$$

$$P^{-1}(\gamma)\widetilde{A}(\gamma) + \widetilde{A}(\gamma)P^{-1}(\gamma) - P^{-1}(\lambda) + P_0^{-1} + \textstyle\sum_i \tau_i \gamma_i^2 I < 0 \quad \forall \quad (\gamma, \lambda) \in \Gamma \times \Lambda \tag{3.63}$$

Bara et al.[27] explains that inequalities Eq. (3.62) and Eq. (3.63) imply the condition that $\mathcal{V}_{convex}\left(\vec{x}(t), \vec{\sigma}(t), \dot{\vec{\sigma}}(t)\right) < 0$ and $P^{-1}(\vec{\sigma}(t)) > 0$, while Eq. (3.61) is a constraint that restricts the choice of $P^{-1}(\vec{\sigma}(t))$. This proves that inequality Eq. (3.38) implies AQS conditions for the generalized LPV system for all parameter variations bounded by Eq. (3.33). A similar methodology is used for the proof of inequality Eq. (3.39), and is presented in more detail in Bara et al.[27].

3.4.7 Adaptive Controller Derivation/Proof

Following the PD-type controller derivation, we will consider only the rotational subsystem for the design of the adaptive controller. The translational input of the controller will be the same as the one designed for the PD-type controller. The state and input vectors are then, $\vec{x}_r(t) = [\psi(t), \theta(t), \phi(t), \omega_x(t), \omega_y(t), \omega_z(t)]^T$ and $\vec{u}_r(t) = [U_x(t), U_y(t), U_z(t)]^T$. We will then redefine the moment applied to the z-axis of our launch vehicle to be $\vec{M}^B(t) = U_z(t) + \Theta$. This changes our linearized rotational equations of motion from Eq. (3.20) to,

$$\begin{aligned}
\dot{\omega}_x(t) &= -\frac{\dot{m}}{m(t)}\omega_x(t) + \frac{U_x(t)}{m(t)\left(\frac{1}{4}r^2 + \frac{1}{12}l^2\right)} \\
\dot{\omega}_y(t) &= -\frac{\dot{m}}{m(t)}\omega_y(t) + \frac{U_y(t)}{m(t)\left(\frac{1}{4}r^2 + \frac{1}{12}l^2\right)} \\
\dot{\omega}_z(t) &= -\frac{\dot{m}}{m(t)}\omega_z(t) + \frac{\Theta}{m(t)\left(\frac{1}{2}r^2\right)} + \frac{U_z(t)}{m(t)\left(\frac{1}{2}r^2\right)}
\end{aligned} \tag{3.64}$$

where, Θ is an unknown constant parameter. By adding the unknown constant parameter to the linearized rotational equations of motion we are able to design a controller to compensate

for an unknown torque generated by the hybrid swirl combustion engine about the z-axis of the launch vehicle. The adaptive controller is then designed by using Lyapunov's Direct Method for nonautonomous systems. For this, we will have to define a new state vector for the system, $\vec{z}_r(t) = [\psi(t), \theta(t), \phi(t), \omega_x(t), \omega_y(t), \omega_z(t), e_\Theta(t)]^T$, where $e_\Theta(t)$ is the unknown parameter estimation error, and is defined as, $e_\Theta(t) = \Theta - \hat{\Theta}(t)$. We start by selecting the candidate Lyapunov function to be the positive definite quadratic function,

$$V(\vec{z}_r(t), t) = \frac{1}{2}\vec{z}_r^T(t) P \vec{z}_r(t)$$

where, $P = I^{7\times 7}$. Expanding the candidate Lyapunov function, we find that,

$$V(\vec{z}_r(t), t) = \frac{1}{2}\psi^2(t) + \frac{1}{2}\theta^2(t) + \frac{1}{2}\phi^2(t) + \frac{1}{2}\omega_x^2(t) + \frac{1}{2}\omega_y^2(t) + \frac{1}{2}\omega_z^2(t) + \frac{1}{2}e_\Theta^2(t)$$

The derivative of the candidate Lyapunov function then follows as,

$$\begin{aligned}\dot{V}(\vec{z}_r(t), t) = {} & \psi(t)\omega_x(t) + \theta(t)\omega_y(t) + \phi(t)\omega_z(t) - \frac{\dot{m}}{m(t)}\omega_x^2(t) - \frac{\dot{m}}{m(t)}\omega_y^2(t) - \frac{\dot{m}}{m(t)}\omega_z^2(t) \\ & + \frac{\omega_x(t)}{m(t)\left(\frac{1}{4}r^2 + \frac{1}{12}l^2\right)}U_x(t) + \frac{\omega_y(t)}{m(t)\left(\frac{1}{4}r^2 + \frac{1}{12}l^2\right)}U_y(t) + \frac{\omega_z(t)}{m(t)\left(\frac{1}{2}r^2\right)}e_\Theta(t) \\ & + \frac{\omega_z(t)}{m(t)\left(\frac{1}{2}r^2\right)}\hat{\Theta}(t) + \frac{\omega_z(t)}{m(t)\left(\frac{1}{2}r^2\right)}U_z(t) - e_\Theta(t)\dot{\hat{\Theta}}(t)\end{aligned}$$

Here, $\dot{e}_\Theta(t) = -\dot{\hat{\Theta}}(t)$ since Θ is constant. Designing the adaptive update law to be,

$$\dot{\hat{\Theta}}(t) = \frac{\omega_z(t)}{m(t)\left(\frac{1}{2}r^2\right)} \tag{3.65}$$

provides us with,

$$\dot{V}\left(\vec{z}_r\left(t\right),t\right)=\psi\left(t\right)\omega_x\left(t\right)+\theta\left(t\right)\omega_y\left(t\right)+\phi\left(t\right)\omega_z\left(t\right)-\frac{\dot{m}}{m\left(t\right)}\omega_x^2\left(t\right)-\frac{\dot{m}}{m\left(t\right)}\omega_y^2\left(t\right)-\frac{\dot{m}}{m\left(t\right)}\omega_z^2\left(t\right)$$
$$+\frac{\omega_x\left(t\right)}{m\left(t\right)\left(\frac{1}{4}r^2+\frac{1}{12}l^2\right)}U_x\left(t\right)+\frac{\omega_y\left(t\right)}{m\left(\frac{1}{4}r^2+\frac{1}{12}l^2\right)}U_y\left(t\right)+\frac{\omega_z\left(t\right)}{m\left(t\right)\left(\frac{1}{2}r^2\right)}\hat{\Theta}\left(t\right)$$
$$+\frac{\omega_z\left(t\right)}{m\left(t\right)\left(\frac{1}{2}r^2\right)}U_z\left(t\right)$$

We can then design the controller, $u_r(t)$, to be,

$$u_r\left(t\right)=\begin{bmatrix}U_x\left(t\right)\\U_y\left(t\right)\\U_z\left(t\right)\end{bmatrix}=\begin{bmatrix}\left(\frac{1}{4}r^2+\frac{1}{12}l^2\right)\left(\dot{m}\omega_x\left(t\right)-m\left(t\right)\psi\left(t\right)-\omega_x\left(t\right)m\left(t\right)\right)\\\left(\frac{1}{4}r^2+\frac{1}{12}l^2\right)\left(\dot{m}\omega_y\left(t\right)-m\left(t\right)\theta\left(t\right)-\omega_y\left(t\right)m\left(t\right)\right)\\\left(\frac{1}{2}r^2\right)\left(\dot{m}\omega_z\left(t\right)-m\left(t\right)\phi\left(t\right)-\hat{\Theta}\left(t\right)-\omega_z\left(t\right)m\left(t\right)\right)\end{bmatrix}\tag{3.66}$$

This controller provides the following Lyapunov function derivative,

$$\dot{V}\left(\vec{z}_r\left(t\right),t\right)=-\omega_x^2\left(t\right)-\omega_y^2\left(t\right)-\omega_z^2\left(t\right)$$

We can now show that $\dot{V}\left(\vec{z}_r\left(t\right),t\right)$ can be upper bounded by the negative of the positive definite radially unbounded continuous function,

$$W_3\left(\vec{z}_r\left(t\right)\right)=-\frac{1}{2}\omega_x^2\left(t\right)-\frac{1}{2}\omega_y^2\left(t\right)-\frac{1}{2}\omega_z^2\left(t\right)$$

Since a positive definite quadratic Lyapunov function is always positive definite decrescent [28], and $\dot{V}\left(\vec{z}_r\left(t\right),t\right)\leq-W_3\left(\vec{z}_r\left(t\right)\right)\leq 0\ \forall\ \omega_x(t),\ \omega_y(t),\ \omega_z(t)\in\mathbb{R}^n, t\geq 0$ the states of $\vec{x}_r(t)$ are shown to be bounded, along with $\hat{\Theta}(t)$, and therefore $e_\Theta(t)$. We will now use Barbalat's Lemma to prove the stability of the system. The second time-derivative of the candidate Lyapunov function follows as,

$$\ddot{V}\left(\vec{z}_r(t),t\right)=2\omega_x\left(t\right)\psi\left(t\right)+2\omega_x^2\left(t\right)+2\omega_y\left(t\right)\theta\left(t\right)+2\omega_y^2\left(t\right)+2\omega_z\left(t\right)\phi\left(t\right)+\frac{2\omega_z\left(t\right)e_\Theta\left(t\right)}{m\left(t\right)}+2\omega_z^2\left(t\right)$$

Since the states of $\vec{z}_r(t)$ were shown to be bounded by $\dot{V}(\vec{z}_r(t))$, and $m(t)$ is defined by Eq. (3.1), we are able to conclude that $\ddot{V}(\vec{z}_r(t))$ is bounded. Therefore, we can state that $\dot{V}(\vec{z}_r(t))$ is uniformly continuous and $\dot{V}(\vec{z}_r(t)) \to 0$ as $t \to \infty$. From Barbalat's Lemma, it follows that $\vec{x}_r(t) \to 0$ as $t \to \infty$. Therefore, we can conclude that the system is made uniformly asymptotically stable by the controller and adaptive update law defined by Eq. (3.66) and Eq. (3.65), respectively.

4 Numerical Simulation Results and Discussion

The four controllers are implemented in MATLAB utilizing the six-degree-of-freedom nonlinear rigid body equations of motion (Eq. (3.6) through Eq. (3.10)). The simulations were run for thirty seconds (the burn time of the launch vehicle) and model the nonlinear dynamics of the launch vehicle with one controller of the four controllers applied at a time. Figure 4.1 presents the scenario that is considered for this research, where an off-nominal internal moment, $\vec{M}_{swirl}$, and an external disturbance force, $\vec{F}_{disturbance}$, act on the launch vehicle.

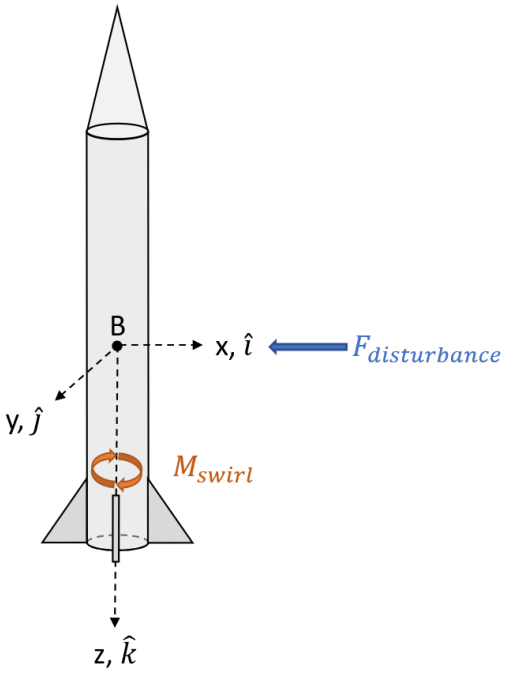

Figure 4.1 Simulation Scenario

$\vec{M}_{swirl}$ and $\vec{F}_{disturbance}$ are modeled in the simulation as nonzero initial conditions. $\vec{M}_{swirl}$ takes the form of $\omega_{z_0} = 1$ rad/s and $\vec{F}_{disturbance}$ takes the form of $v_{x_0} = 10$ m/s. The desired states of the system are $\vec{x}_{desired}(t) = [0, 0, -200, 0, 0, 0, 0, 0, -200 \times t, 0, 0, 0]^T$ with no acceleration.

Figure 4.2 presents the dynamic model of the launch vehicle when the LQR controller is

applied, were $Q = diag([1, 1, 1, 1, 1, 1, 1, 1, 1, 10000, 10000, 1]) \times 10^5$, and $R = I^{6\times6} \times 10^{-2}$. From this figure, it is clear that the LQR controller was able to achieve the goal of stabilizing the launch vehicle before the end of the main engine burn.

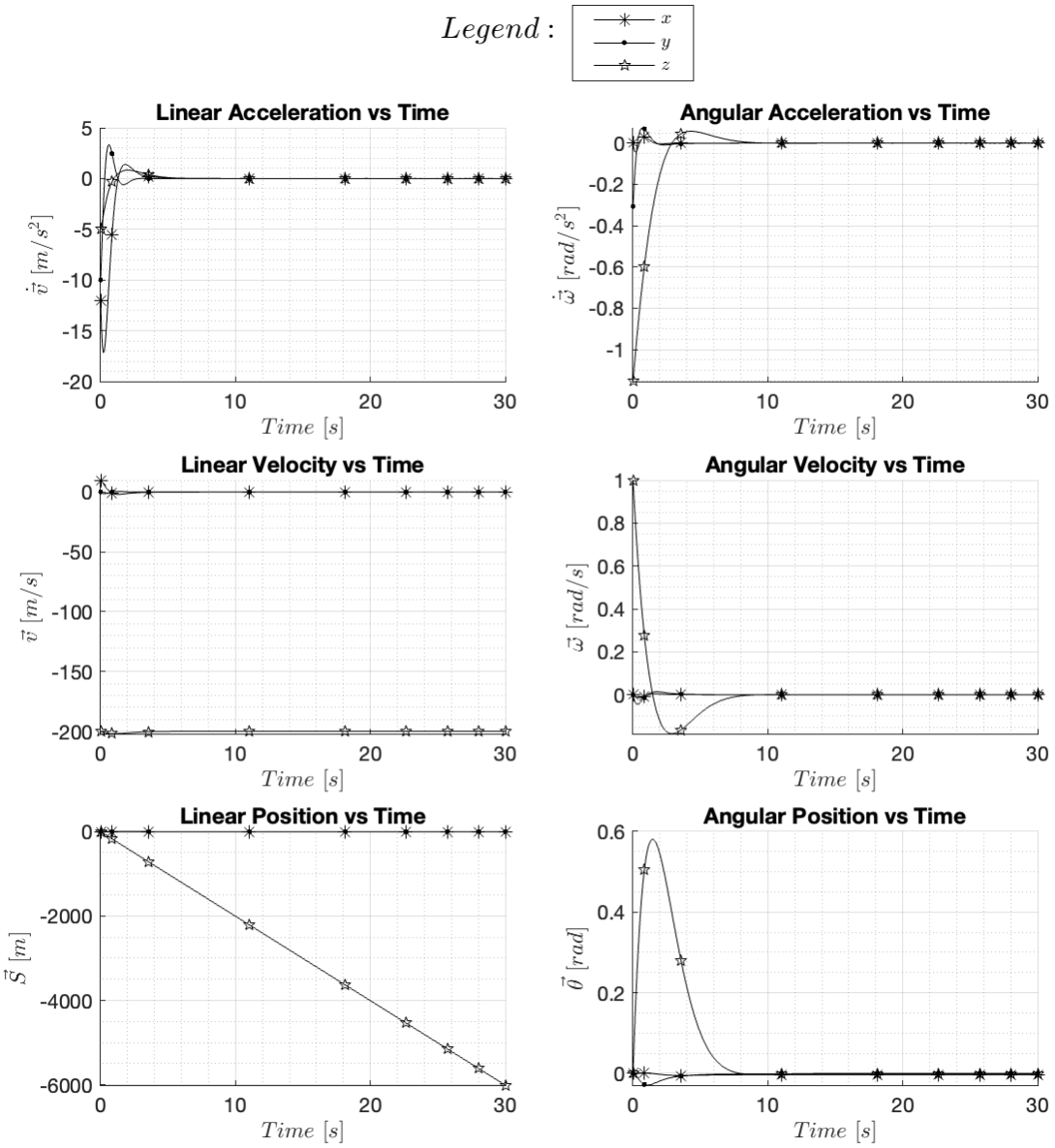

Figure 4.2 LQR Controller

Figure 4.3 presents the dynamic model of the launch vehicle when the PD-type controller is applied. From this figure, it is shown that the PD-type controller also achieved the goal of stabilizing the launch vehicle within the thirty second burn time of the main engine.

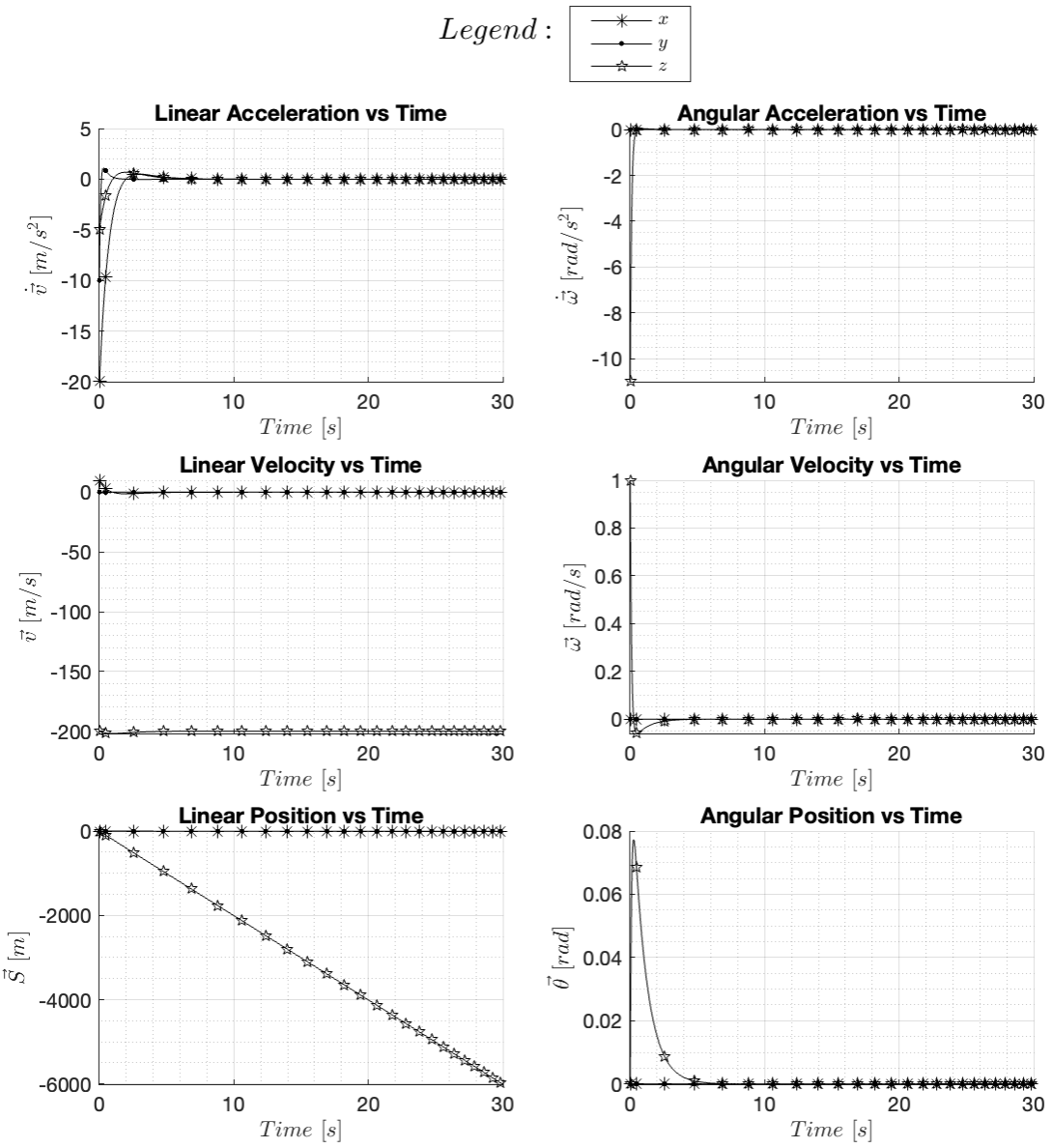

Figure 4.3 PD-Type Controller

Figure 4.4 presents the simulation results for the affine parameter-dependent Lyapunov function based controller where a weighing matrix of $K_{weigh} = diag([1, 1, 1, 10, 10, 10, 1, 1, 1, 100, 100, 100])$ was multiplied to the controller gain, $K(\vec{\sigma}(t))$, to make the affine parameter-dependent Lyapunov function based controller more aggressive.

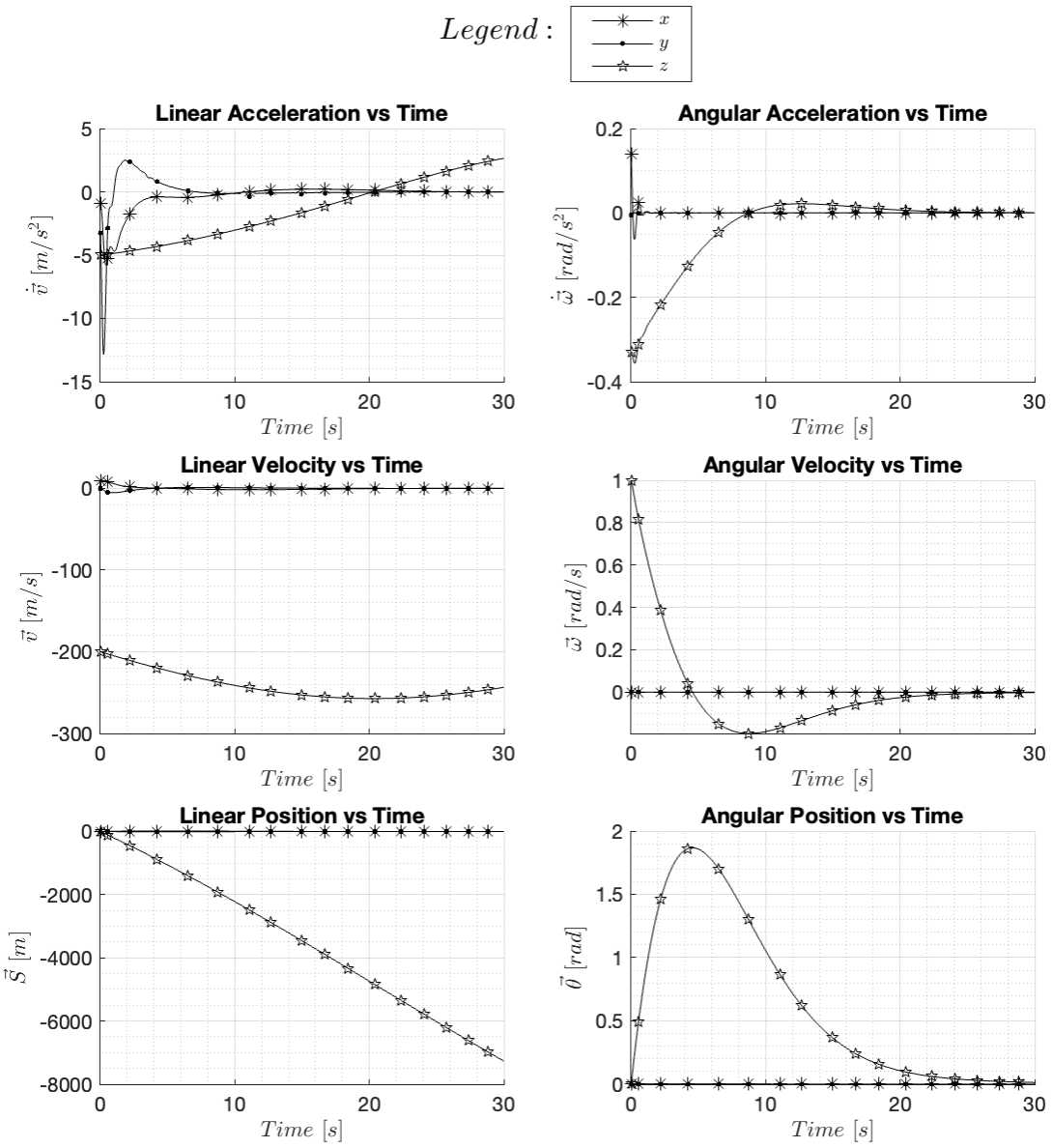

Figure 4.4 Affine Parameter-Dependent Lyapunov Function Based Controller

From Figure 4.4 it is clear that the affine parameter-dependent Lyapunov function based controller nearly achieved the goal of stabilizing the launch vehicle within the thirty second burn time of the main engine. It is believed that the affine parameter-dependent Lyapunov function based controller was not able to meet the stability goals of this research since it is an optimal control approach; therefore the controller is not necessarily able to stabilize the launch vehicle quickly enough to meet the thirty second requirement even after making the

controller more aggressive with the weighing matrix. Additionally, it is difficult to tune the gains of this controller to make it more aggressive because the Lyapunov conditions must be satisfied for both the upper and lower bound of the uncertain parameter, which greatly limits the choice of gains.

Next, Figure 4.5 presents the simulation results for the adaptive controller. From this figure it is clear that the adaptive controller was able to meet the stability goal of this research.

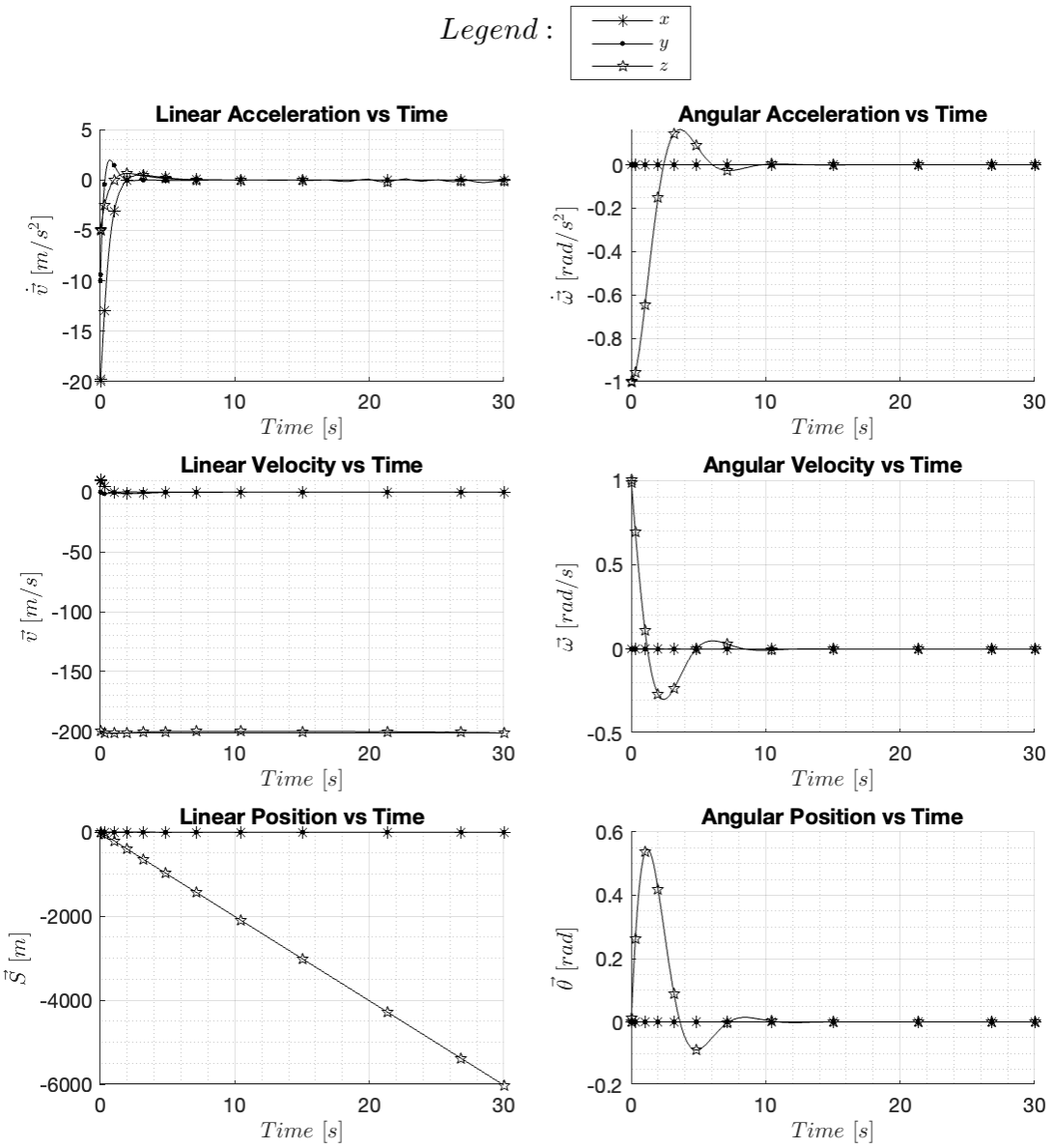

Figure 4.5 Adaptive Controller

Lastly, Figure 4.6 presents the vector 2-norm of the control vector, $\vec{u}(t)$ for each of the four controllers, where the first five seconds of the simulation are shown in more detail in Figure 4.7.

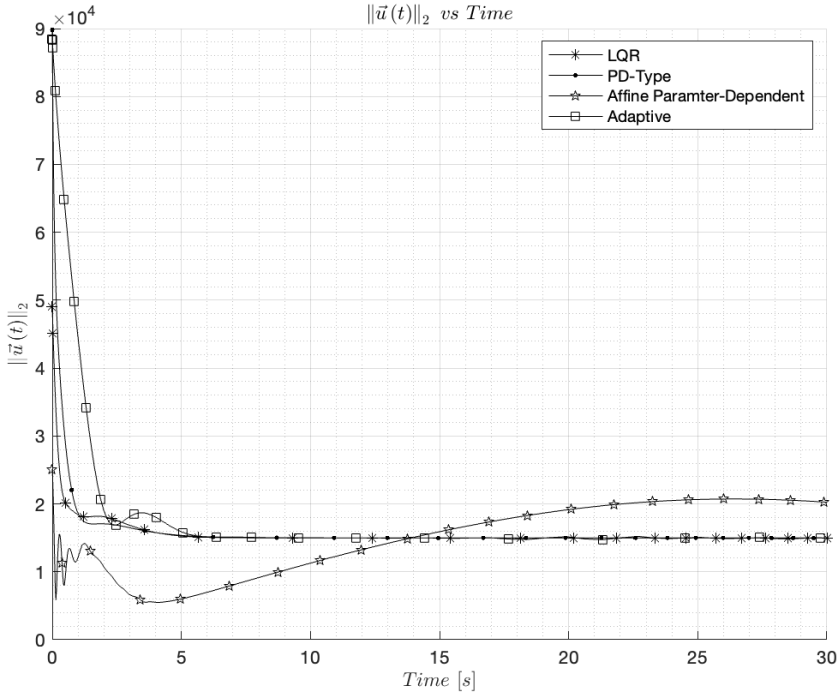

Figure 4.6 $\|\vec{u}(t)\|_2$ vs Time

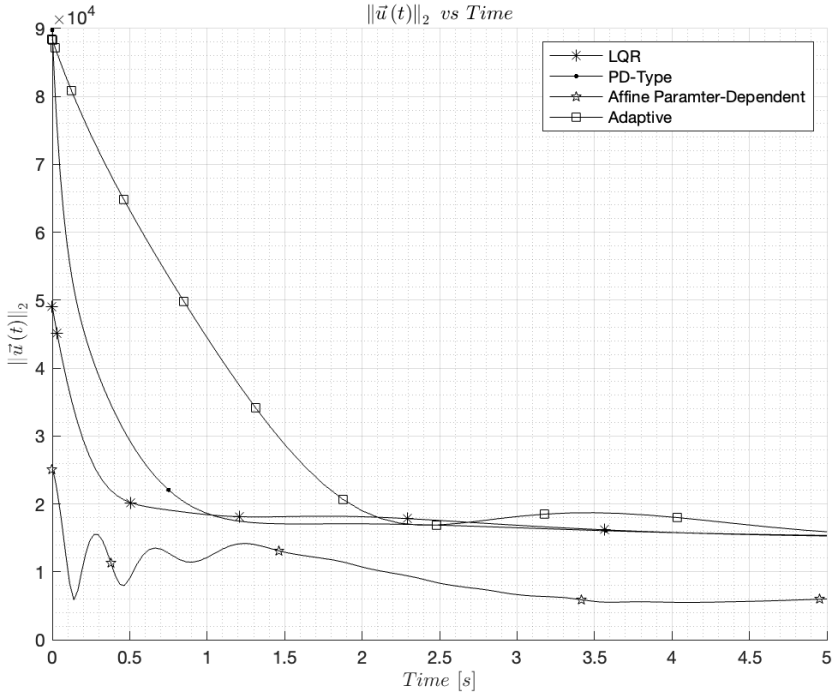

Figure 4.7 $\|\vec{u}(t)\|_2$ vs Time (0 to 5 Seconds)

From Figure 4.7 it is shown that the LQR controller used less control effort than the PD-type and adaptive controllers. Therefore, depending on the application, either the LQR controller or the PD-type controller may be considered the best performing controller, since the LQR controller used less control effort, while the PD-type controller stabilized the system in the shortest amount of time. Additionally, from Figure 4.7 it is shown that the affine parameter-dependent Lyapunov function based controller exerted considerably less control effort than the other three controllers for the first $\approx$ 14 seconds of the simulation. This reinforces the earlier statement that the controller needs to be made more aggressive to stabilize the launch vehicle within the main engine's burn time.

5 Conclusions and Recommendation

This research designed a new system model and proposed four solutions for controlling a launch vehicle with an internally originating torque. These controllers include an LQR controller, a PD-type controller, an affine parameter-dependent Lyapunov function based controller, and an adaptive controller.

One of the early conclusions of this research was that the location of the center of mass of a hybrid rocket engine powered launch vehicle only changes a small amount. Therefore, it is shown that this change in location can be neglected for the subsequent equation of motion derivations. After the equations of motion were derived and the simulations were run, it was shown that, although the affine parameter-dependent Lyapunov function based controller was not able to stabilize the launch vehicle within the thirty second burn time of the main engine, this research did achieve its goals by designing three simple and robust controllers which are able to stabilize a launch vehicle with an internally originating torque within the main engine's burn time. This research concluded that, since the affine parameter-dependent Lyapunov function based controller is an optimal control approach, there is no guarantee that it has the ability to stabilize the launch vehicle quickly enough to meet the thirty second requirement. Additionally, this controller is not recommended due to the limited choice of stabilizing gains. Therefore, due to their simplicity, and ability to stabilize a swirl combustion hybrid rocket engine powered launch vehicle within the main engine's burn time, this thesis recommends the use of either the LQR controller or the PD-type controller. Depending on the application, either the LQR controller will be preferred due to its low control effort, or the PD-type controller will be preferred due to its ability to quickly stabilize the system. It should be noted that this conclusion assumes there to be no noise in the system. A controller that takes the derivative of a noisy signal may cause the controller to perform unsatisfactory. Therefore, this is a potential concern for the PD-type controller.

This work may be extended by the acquisition of mathematical models for the dynamic behavior of swirl combustion hybrid launch vehicle engines with internally originating torque.

These models would hopefully provide enough data to relate the thrust of the engine to the corresponding torque produced. This data would improve the accuracy of our models and aid in the design of future controllers. Additionally, this data would allow us to begin adding other complexities to our model, such as engine throttling and trajectory tracking.

REFERENCES

[1] Jones, C. C., "Performance and Analysis of Vortex Oxidizer Injection in a Hybrid Rocket," Tech. rep., NAVAL ACADEMY ANNAPOLIS MD, 2009.

[2] Wallace, K. M., "Linear throttling high regression rate vortex flow field injection system within a hybrid rocket engine," , Feb. 27 2020. US Patent App. 16/550,063.

[3] Vortex, S. O., and Rocket, *Sierra Nevada Corporation*, 2015. November 10. October 01, 2020.

[4] Gomes, S., Rocco, L., and Rocco, J., "Swirl Injection Effects on Hybrid Rocket Motors," *Journal of Aerospace Technology and Management*, Vol. 7, 2015, pp. 418–424.

[5] Motoe, M., Matsuno, T., and Shimada, T., "Numerical analysis of combustion field in hybrid rocket motor with swirling and axial oxidizer injection," *7th European Conference for Aeronautics and Space Sciences*, 2017.

[6] Heydari, M. M., and Massoom, N. G., "Experimental Study of the Swirling Oxidizer Flow in HTPB/N2O Hybrid Rocket Motor," *International Journal of Aerospace Engineering*, 2017.

[7] Kinzie, R., and Seo, D., "Controller Design for Launch Vehicle with Internal Torque," 2021.

[8] Du, W., *Dynamic modeling and ascent flight control of Ares-I Crew Launch Vehicle*, Iowa State University, 2010.

[9] Zipfel, P., *Introduction to Tensor Flight Dynamics*, 2019.

[10] Zipfel, P. H., *Modeling and simulation of aerospace vehicle dynamics*, Aiaa, 2000.

[11] Zipfel, P., *Modeling INS/GPS/Star-Traker in 6 DoF*, 2015.

[12] Fleeman, E., *Missile design and system engineering*, American Institute of Aeronautics and Astronautics, Inc., 2012.

[13] Moon, J., and Başar, T., "Robust control of LTI systems over unreliable communication channels with unreliable acknowledgments," *2016 IEEE Region 10 Conference (TENCON)*, 2016, pp. 3390–3393. https://doi.org/10.1109/TENCON.2016.7848682.

[14] Stengel, R. F., and Ryan, L. E., "Stochastic robustness of linear time-invariant control systems," *IEEE Transactions on Automatic Control*, Vol. 36, No. 1, 1991, pp. 82–87. https://doi.org/10.1109/9.62270.

[15] Kwakernaak, H., *Linear optimal control systems*, Wiley Interscience, New York, 1972.

[16] Chen, C., "On the Robustness of the Linear Quadratic Regulator via Perturbation Analysis of the Riccati Equation," *School of Electronic Engineering Dublin City University*, 2014.

[17] Hespanha, J. P., "Undergraduate Lecture Notes on LQG/LQR controller design," *University of California, Santa Barbara*, 2007.

[18] Yang, Y., "Quaternion-Based LQR Spacecraft Control Design Is a Robust Pole Assignment Design," *Journal of Aerospace Engineering*, Vol. 27, 2014.

[19] Yang, Y., "Analytic LQR Design for Spacecraft Control System Based on Quaternion Model," *Journal of Aerospace Engineering*, Vol. 25, 2012.

[20] Doyle, J., "Robust and optimal control," *35th Conference on Decision and Control*, 1996.

[21] Zaffar, S., and Memon, A. Y., "Robust and optimal stabilization of uncertain linear systems using LQR methods," *2014 UKACC International Conference on Control (CONTROL)*, 2014, pp. 163–167. https://doi.org/10.1109/CONTROL.2014.6915133.

[22] Shahruz, S. M., Langari, G., and Tomizuka, M., "Design of Robust PD-Type Control Laws for Robotic Manipulators with Parametric Uncertainties," *1992 American Control Conference*, 1992, pp. 2967–2968. https://doi.org/10.23919/ACC.1992.4792690.

[23] Wang, L., Li, M., and Yang, H., "Robust PD-Type Iterative Learning Control of Discrete Linear Repetitive Processes in the Finite Frequency Domain," *Mathematics*, Vol. 8, No. 6, 2020, p. 1004. https://doi.org/10.3390/math8061004.

[24] Visioli, A., and Zhong, Q.-C., *PID–PD Control*, chapter and pages, pp. 121–140. https://doi.org/10.1007/978-0-85729-070-0-7.

[25] Sandiwan, A. P., Cahyadi, A., and Herdjunanto, S., "Robust proportional-derivative control on SO(3) with disturbance compensation for quadrotor UAV," *International Journal of Control, Automation and Systems*, Vol. 15, No. 5, 2017, pp. 2329–2342. https://doi.org/10.1007/s12555-016-0452-5.

[26] Leith, D., and Leithead, W., "Survey of gain-scheduling analysis and design," *International journal of control*, Vol. 73, No. 11, 2000, pp. 1001–1025.

[27] Bara, G., Daafouz, J., and Ragot, J., "Gain scheduling techniques for the design of observer state feedback controllers," *IFAC Proceedings Volumes*, Vol. 35, 2002, pp. 13–18.

[28] Khalil, H. K., "Nonlinear systems third edition," *Prentice Hall*, Vol. 115, 2002.

[29] Nguyen, N. T., "Model-reference adaptive control," *Model-Reference Adaptive Control*, Springer, 2018.

[30] Barfoot, T., Forbes, J. R., and Furgale, P. T., "Pose estimation using linearized rotations and quaternion algebra," *Acta Astronautica*, Vol. 68, No. 1-2, 2011, pp. 101–112. https://doi.org/10.1016/j.actaastro.2010.06.049.

[31] The MathWorks, I., "Control System Toolbox," *MATLAB*, 2020, pp. 687, 688.

[32] van de Geijn, R., and Myers, M., "Advanced linear algebra: Foundations to frontiers," *Creative Commons NonCommercial (CC BY-NC)*, 2020.

[33] Duan, G.-R., and Patton, R. J., "A note on Hurwitz stability of matrices," *Automatica*, Vol. 34, No. 4, 1998, pp. 509–511.

[34] Gahinet, P., Apkarian, P., and Chilali, M., "Affine parameter-dependent Lyapunov functions and real parametric uncertainty," *IEEE Transactions on Automatic control*, Vol. 41, No. 3, 1996, pp. 436–442.

[35] Boyd, S., Ghaoul, L. E., and Feron, E., *Linear Matrix Inequalities in System and Control Theory*, CAMBRIDGE, 1987. URL https://www.ebook.de/de/product/23735754/stephen_boyd_laurent_el_ghaoul_eric_feron_linear_matrix_inequalities_in_system_and_control_theory.html.

[36] Haynsworth, E. V., "ON THE SCHUR COMPLEMENT." Tech. rep., 1968.